

ISTANBUL TECHNICAL UNIVERSITY ★ GRADUATE SCHOOL OF SCIENCE
ENGINEERING AND TECHNOLOGY

**RESILIENT ULTRA DENSE NETWORKS
UNDER UAV COVERAGE FOR DISASTER MANAGEMENT**



Ph.D. THESIS

Elif BOZKAYA

Department of Computer Engineering

Computer Engineering Programme

JULY 2020

ISTANBUL TECHNICAL UNIVERSITY ★ GRADUATE SCHOOL OF SCIENCE
ENGINEERING AND TECHNOLOGY

**RESILIENT ULTRA DENSE NETWORKS
UNDER UAV COVERAGE FOR DISASTER MANAGEMENT**



Ph.D. THESIS

**Elif BOZKAYA
(504152506)**

Department of Computer Engineering

Computer Engineering Programme

Thesis Advisor: Assoc. Prof. Dr. Berk CANBERK

JULY 2020

**AFET YÖNETİMİNDE İHA'LAR İLE
DAYANIKLI ULTRA YOĞUN AĞLAR**

DOKTORA TEZİ

**Elif BOZKAYA
(504152506)**

Bilgisayar Mühendisliği Anabilim Dalı

Bilgisayar Mühendisliği Programı

Tez Danışmanı: Assoc. Prof. Dr. Berk CANBERK

TEMMUZ 2020

Elif BOZKAYA, a Ph.D. student of ITU Graduate School of Science Engineering and Technology student ID 504152506 successfully defended the thesis entitled “RE-SILIENT ULTRA DENSE NETWORKS UNDER UAV COVERAGE FOR DISASTER MANAGEMENT”, which she prepared after fulfilling the requirements specified in the associated legislations, before the jury whose signatures are below.

Thesis Advisor : **Assoc. Prof. Dr. Berk CANBERK**
Istanbul Technical University

Jury Members : **Prof. Dr. Sema Fatma OKTUĞ**
Istanbul Technical University

Prof. Dr. Lütfiye DURAK ATA
Istanbul Technical University

Assoc. Prof. Dr. Didem GÖZÜPEK
Gebze Technical University

Assoc. Prof. Dr. Müge SAYIT
Ege University

Date of Submission : **26 May 2020**

Date of Defense : **21 July 2020**





To my family,



FOREWORD

I would like to thank my advisor, Assoc. Prof. Dr. Berk Canberk, for giving me the opportunity to pursue this doctorate, and spending a lot of time talking to me about ideas that led up to this work. I cannot thank him enough for his patience and guidance that helped me grow as an independent researcher. This work has taught me many valuable skills that I will be able to apply in future ventures. I would like to also thank the research group, The Broadband Communication Research Group, BCRG, for being such a great place to study during my MSc and PhD periods in the Computer Engineering Department of Istanbul Technical University.

I also give sincere thanks to Prof. Dr. Stefan Schmid from the University of Vienna for his valuable insights and supervising my study during my visiting period. Along with him, all the team members of the Research Group Communication Technologies were more than welcoming and collaborative, making my visit a valuable experience.

I am also immensely grateful to my thesis committee Prof. Dr. Sema Fatma Oktuğ and Assoc. Prof. Dr. Didem Gözüpek who gave me numerous suggestions and took time to provide me guidance about the thesis.

I would like to acknowledge and thank The Scientific and Technical Research Council of Turkey (TUBITAK) for their support through 2214 International Research Fellowship Programme (for PhD Student) and I would also like to acknowledge The Scientific and Technical Research Council of Turkey (TUBITAK) 1001 The Scientific and Technological Research Projects Funding Program with project number 119E434 for their support.

Most importantly, none of this would have been possible without the support and patience of my family. My heartfelt and deepest thanks, to my family. I also owe special thanks to my friend Dr. Ece Elvan Kartal, for her continuous support and encouragement.

July 2020

Elif BOZKAYA
(Computer Engineer, M.Sc.)

TABLE OF CONTENTS

	<u>Page</u>
FOREWORD.....	ix
TABLE OF CONTENTS.....	xi
ABBREVIATIONS	xiii
SYMBOLS	xv
LIST OF TABLES	xvii
LIST OF FIGURES	xix
SUMMARY	xxi
ÖZET	xxiii
1. INTRODUCTION	1
1.1 Purpose and Scope of the Thesis	4
1.2 Thesis Overview	6
2. LITERATURE REVIEW.....	7
2.1 Resilience in Communication Networks	7
2.2 Coverage Problem and ABS Deployment	9
2.3 Maximizing Flight Endurance.....	9
2.4 Path planning	10
2.5 Handover Management.....	11
3. NETWORK ARCHITECTURE AND MODEL.....	13
3.1 Network Model.....	15
3.2 Architectural Model.....	18
4. AirNet SYSTEM.....	19
4.1 Optimal ABS Deployment	19
4.2 Demand-Aware Reconfiguration	24
4.3 Endurance Framework.....	26
4.4 Path Planning.....	28
4.5 Scheduling between ABSs and Replenishment Stations.....	30
4.6 Handover Procedure	33
4.6.1 Markov decision process	33
4.6.2 TD learning prediction: Q-learning.....	36
4.6.3 Handover decision	37
4.6.3.1 ABS transition probability estimation	38
4.6.4 Handover execution	40
5. EVALUATION OF THE STUDY	41
5.1 Simulation Setup	41
5.2 Benefits of Energy-Efficient Deployment	42
5.3 Demand-Aware Reconfiguration	44
5.4 Benefits of Scheduling.....	45

5.5 Handover Procedure	48
6. CONCLUSION	51
REFERENCES.....	53
APPENDICES.....	59
APPENDIX A: Proof of Approximations	61
CURRICULUM VITAE.....	66



ABBREVIATIONS

2D	: Two Dimensional
3D	: Three Dimensional
3GPP	: The 3rd Generation Partnership Project
A2A	: Air to Air
A2G	: Air to Ground
ABS	: Aerial Base Station
API	: Application Program Interface
AUVSI	: Association for Unmanned Vehicle Systems International
BS	: Base Station
DRL	: Deep Reinforcement Learning
EPC	: Evolved Packet Core
GPS	: Global Positioning System
LoS	: Line of Sight
LTE	: Long Term Evolution
NLoS	: Non-Line of Sight
NP	: Non-Polynomial
NRT	: Non-Real Time
PDF	: Probability Density Function
QoE	: Quality of Experience
QoS	: Quality of Service
RAN	: Radio Access Network
RAT	: Radio Access Technology
RWP	: Random Waypoint
RB	: Resource Block
RL	: Reinforcement Learning
RSRP	: Reference Signal Received Power
RSSI	: Received Signal Strength Indicator
S1AP	: S1 Application Protocol
SDN	: Software Defined Networking
SINR	: Signal to Interference and Noise
SITL	: Software in the Loop
TD	: Temporal-Difference
TTT	: Time to Trigger
UAV	: Unmanned Aerial Vehicle
UDN	: Ultra Dense Network
UE	: User Equipment



SYMBOLS

M	: Number of ABSs in the network
$R_{cluster}$: Coverage radius of an ABS
h_j	: Altitude of ABS_j
U	: Number of UEs
A	: The size of target area (Note that a is the length of one side of the square)
$t_1 - t_0$: Transiting time from initial location to designated location
$t_2 - t_1$: Hover time
$t_3 - t_2$: Transiting time from designated location to initial location
$P_{cov,i}$: Coverage probability of UE_i
P_t	: Transmission power of ABS
$P_{r,i}$: Received power by UE_i
P_{min}	: Minimum received power
E_{max}	: ABS battery capacity
E_{res,t_y}	: Residual energy level of the ABS at time t_y
E_{con,t_y}	: Consumed energy of the ABS at time t_y
N	: Noise power
I	: Interference received from the nearest ABS
$P(LoS)$: LoS probability
$P(NLoS)$: NLoS probability
$P_{threshold}$: SNIR threshold ratio
η	: Path loss coefficient
$g(\varphi_k)$: Antenna gain
θ	: Elevation angle
f_c	: Carrier frequency
n	: Path loss exponent
ρ	: Air density
m_d	: ABS weight
m	: ABS propeller
v_d	: Average ABS speed
v_{max}	: Maximum ABS speed
P_{hov}	: Hover power
(x_j, y_j, h_j)	: Location of an ABS_j in coordinate system
R_T	: Time to retry on the failure of a handover
R_W	: Waiting time for the establishment of a handover
T_R	: Handover time
μ_{LoS}	: Mean of shadow fading for LoS
σ_{LoS}^2	: Variance of shadow fading for LoS
μ_{NLoS}	: Mean of shadow fading for NLoS
σ_{NLoS}^2	: Variance of shadow fading for NLoS
t_a	: Arrival time of the ABS in the replenishment station
t_d	: Departure time of the ABS in the replenishment station
C	: Capacity of the battery
I_c	: Current of the charge



LIST OF TABLES

	<u>Page</u>
Table 4.1 : Simulation for the allocation 9 RBs with 3 UEs.	26
Table 4.2 : Transition probabilities.....	34





LIST OF FIGURES

	<u>Page</u>
Figure 1.1 : State of packet traffic after 2011 Tohoku earthquake in Japan [1]. ...	2
Figure 1.2 : Considered scenario for aerial networks.	5
Figure 3.1 : Considered scenario for SDN-based aerial networks.	14
Figure 3.2 : OpenFlow table message format.	15
Figure 3.3 : Connection between ABSs and UEs.	15
Figure 3.4 : ABS life cycle.	16
Figure 3.5 : Control architecture.	18
Figure 4.1 : <i>AirNet</i> flow chart.	19
Figure 4.2 : Adjustment of coverage area with a single ABS.	20
Figure 4.3 : Coverage area as result of different altitude of deployed ABSs.	21
Figure 4.4 : Residual energy for two different cases.	23
Figure 4.5 : (a) Coverage area with single ABS ($10^{-4}UEs/m^2$) (b) Coverage areas with 2 ABSs ($2 \times 10^{-4}UEs/m^2$).	24
Figure 4.6 : (a) The relationship between coverage radius, $R_{cluster}$ and altitude (b) Coverage ratio with increasing number of ABSs (c) Consumed transition and hover energy before the first ABS deployment and after the update of location of control station.	25
Figure 4.7 : Illustration of path planning (a) ABS deployment and construction of the weighted graph (b) Possible path planning processes.	29
Figure 4.8 : Recharging requests of ABSs.	31
Figure 4.9 : (a) Illustration of busy period of replenishment station (b) Before scheduling (c) After scheduling.	32
Figure 4.10 : Energy-aware handover mechanism.	34
Figure 4.11 : Transition graph.	35
Figure 4.12 : In the case of ABS battery depletion.	38
Figure 4.13 : Handover procedure with ABS transition probability estimation.	39
Figure 4.14 : Markov chain for the transition probabilities.	39
Figure 5.1 : Simulation environment.	41
Figure 5.2 : Covering a given target area with $M=10$ ($R_{cluster} = 0.2182a(m)$) and $M=15$ ($R_{cluster} = 0.1796a(m)$).	43
Figure 5.3 : ABS deployment for different schemes with 10 ABSs (a) Random ABS deployment (b) ABS deployment to the locations of damaged BS (c) Set cover approach (d) Energy-aware ABS deployment.	44
Figure 5.4 : Coverage utility for 4 different schemes.	45
Figure 5.5 : Consumed transition energy of individual ABSs.	45
Figure 5.6 : Average hover time w.r.t. total throughput.	46
Figure 5.7 : Normalized recharging delay before scheduling and after scheduling with different number of replenishment station.	46

Figure 5.8 : (a) Mean number of ABSs and (b) Mean charging time in the replenishment station. **47**

Figure 5.9 : Probability density function of recharging delay for one ABS. The number of replenishment station is equal to 5, 4, 3 and 2. The number of waiting ABSs is equal to 8. **48**

Figure 5.10: Handover failure ratio w.r.t. user density..... **49**

Figure 5.11: Handover delay (ms) with 20 ABSs w.r.t. varying number of users. **49**



RESILIENT ULTRA DENSE NETWORKS UNDER UAV COVERAGE FOR DISASTER MANAGEMENT

SUMMARY

Resiliency in communication networks is the maintainability of the communication functionality at acceptable levels against possible errors, environmental problems, network outage due to technological causes or malicious attacks. However, it is tremendously time-consuming to redesign the network in a versatile disaster situation considering today's static and conservative communication network infrastructures. In disaster management; assessing the situation, taking immediate and effective precautions and proposing solutions for the optimization is only possible with a robust communication network infrastructure. Additionally, in the case of base station failures, there is no infrastructure to manage the mobile traffic in today's mobile network provider systems. In order to solve this problem, mobile data traffic should be managed adaptively.

In recent years, the disasters which were caused by climatic changes cannot be prevented. In case of a natural disaster, the most important thing is to save people's lives. In a situation like this, the first 72 hours is crucially important to react immediately and this can only be possible with quick and effective search and rescue activities. On the other hand, the lack of awareness and communications will vitiate these activities. For example, after the 2011 Tohoku Earthquake in Japan, most of the base stations became out-of-service and the Internet became available barely after 7 days. Also, the service quality of the satellite phones, which are used only for voice communications by the save and rescue teams had decreased. A similar situation was experienced in 2010 after the earthquake in Haiti and long-term communication problems arose due to damaged service provider infrastructures. Similar natural events in the different habitats of the American continent are repeated every year. In addition, after the Marmara Earthquake in 1999, the communication networks have become completely damaged and unusable. In such cases, the continuity of communication is important. In the mentioned disaster scenarios, it is not possible to meet the data demands with the limited physical resources of the infrastructure along with the damages in the existing wireless communication infrastructure. To this end, novel applications are needed in order to solve the network management problems in case of an unanticipated failure.

Today, with the increasing use of Unmanned Aerial Vehicles (UAV), many new applications are emerging in the communication sector. According to the Association for Unmanned Vehicle Systems International (AUVSI) Report, direct economic impact from the UAV industry in US is about 3.6 Billion Dollar in 2018 and is expected to exceed 5 Billion Dollar by 2025. In this thesis, UAVs are proposed to support the communication infrastructure as Aerial Base Stations (ABS) via a centralized controller to solve the problems for existing network infrastructures. ABSs have become a promising tool for post-disaster communications. ABS deployment assists

terrestrial networks to minimize the disruptions caused by unexpected and temporary situations. Thus, it is aimed to design a resilient network management mechanism with ABSs. ABSs which will be located instead of the failed base stations are advantageous because they have low production and maintenance costs, they have error/damage tolerance and they can easily be controlled and located where humans have limited reach. However, because of the physical limitations with low-capacity power supplies, they have limited flying time, limited velocity and communication range. Moreover, the majority of energy consumption in aerial networks is not spent on computing or communication, but on the power required by engines and flying aerial vehicles. For all these reasons, there are various problems in the system design while trying to accomplish real-world problems and complicated duties. Therefore, in order to increase resiliency in aerial networks, a proper positioning management and a flight planning mechanism are both needed considering the relationship between ABS flight characteristics and energy consumption.

Considering the stated reasons, we first focus on on-demand communication. Since on-demand communication can change over time and be hard to accurately predict, it needs to be handled in an online manner, accounting also for battery consumption constraints. This thesis presents an efficient software-based solution to operate ABSs by meeting these requirements which maximizes the number of covered users, and a scheduler which navigates and recharges ABSs in an energy-aware manner. To this end, we propose an energy-aware deployment algorithm and use an energy model to analyze the power consumption and thereby, improve the flight endurance. In addition, we evaluate a novel scheduling mechanism that efficiently manages the ABSs' operations. Our simulations indicate that our approach can significantly improve the flight endurance and user coverage.

In the second part of the thesis, we consider that the continuity of the service has increased the challenge of providing satisfactory quality of service. The limited battery capacity and vertical movement with direction switching of ABSs result in frequent interruptions with additional problems related to increased interference, handover delay, and failure of the handover procedure. Therefore, the main goal is to model dynamic mobile network topology and create a scalable structure to manage possible handover procedure between ABSs. With this idea, a solution is presented in a flexible and centralized structure, which analyses the resiliency of the network and is sensitive to increased mobile data traffic and dynamic topology changes. We address the handover procedure in aerial networks by integrating a reinforcement based Q-learning framework. The proposed model enables to ABSs to learn the optimal deployment exploring a Temporal-Difference (TD) learning prediction method. Our study gives a centralized handover procedure avoiding additional overhead to the ABSs and the transition probabilities are estimated to decrease the risk of the handover failure ratio.

AFET YÖNETİMİNDE İHA'LAR İLE DAYANIKLI ULTRA YOĞUN AĞLAR

ÖZET

İletişim ağlarında dayanıklılık; hatalara, çevresel problemlere, teknolojiye dayalı kesintilere veya kötü niyetli saldırılara karşı, haberleşmenin işlevselliğini kabul edilebilir bir seviyede devam ettirebilmesidir. Ancak, günümüz iletişim ağları alt yapısının statik ve değişikliklere kolay adapte olamayan bir yapıda olduğu düşünüldüğünde, çok yönlü bir afet durumunda ağı yeniden düzenlemek, çok fazla zaman harcanmasına neden olmaktadır. Bir afet yönetiminde, durum değerlendirmesi, hasarlara karşı hızlı ve etkili önlem alınması, ve etkin iyileştirme mekanizmaları sunulması dayanıklı bir iletişim ağı ile mümkündür. Son yıllarda internete bağlı mobil cihaz sayısının artışıyla birlikte günümüzde aylık ortalama 17 exabytes olan global veri trafiğinin, 2021 yılında aylık ortalama 49 exabytes olması tahmin edilmektedir. Bu şartlar altında, baz istasyonları servis dışı kaldığında, günümüz mobil ağ sistemlerinde, mobil trafik akışını yönetebilecek başka yapılar bulunmamaktadır. Bu problemler, mobil haberleşme ağlarının tek bir noktadan esnek ve dinamik yönetilmemesinden kaynaklanır. Bu sorunu çözebilmek için, mobil veri trafiğinin adaptif bir şekilde yönetilmesi gerekmektedir.

Son yıllarda iklimsel değişikliklerle meydana gelen afetler önlenememektedir. Bir doğal afet meydana geldiğinde, en önemli konu insan hayatlarının korunmasıdır. Böyle durumlarda, arama ve kurtarma çalışmalarının büyük oranda başarıya ulaştığı ilk 72 saat oldukça kritik bir zaman dilimidir. Diğer yandan, iletişimde ve durumsal farkındalıkta meydana gelebilecek eksiklikler, kurtarma görevlerinin etkinliğini azaltmaktadır. Örneğin, 2011 Japonya depreminden sonra, 4 gün boyunca baz istasyonlarının çoğu devre dışı kalmış ve ancak 7. günün sonunda İnternet servisi verilmeye başlanmıştır. Kurtarma ekipleri tarafından sadece ses için kullanılan uydu telefonlarının servis kalitesinde sıkıntılar yaşanmıştır. Benzer bir durum, 2010 yılında Haiti'deki deprem sonrasında da yaşanmıştır ve hasar gören servis sağlayıcı alt yapıları nedeniyle uzun süreli iletişim problemi ortaya çıkmıştır. Amerika kıtasının farklı yaşam alanlarında benzer doğa olayları her yıl tekrarlanmaktadır. Ayrıca, yaşadığımız coğrafyada Marmara depremi sonrası, iletişim ağları tamamen hasar görmüş ve kullanılamaz hale gelmiştir. Belirtilen felaket senaryolarında, mevcut kablosuz haberleşme altyapısında meydana gelen hasarlarla birlikte, altyapının kısıtlı fiziksel kaynaklarıyla veri taleplerinin karşılanması mümkün değildir. Bu maksatla, artan mobil trafik akışını ve baz istasyonlarının servis dışı kalması ile ortaya çıkan ağ yönetim sorunlarını çözmek için yeni uygulamalara ihtiyaç duyulmaktadır.

Bu maksatla, bu çalışmada İnsansız Hava Araçlarının iletişim altyapısını desteklemek için kullanımı önerilmektedir. Servis dışı kalan baz istasyonlarının yerine havasal baz istasyonları son kullanıcılara hizmet verebilirler. Bu çalışmada amaç, felakete dayalı senaryolara karşı havasal baz istasyonları ile dayanıklı bir iletişim ağı tasarlamaktır. Dayanıklı ağ ise, afet yönetiminde havasal ağlarda meydana gelen ve iletişim ağlarını

etkileyebilecek problemlere karşı iletişim ağının işlevselliğini kabul edilebilir bir seviyede devam ettirebilmesi olarak tanımlanmıştır.

Bunun yanında, havasal baz istasyonların dayanıklı bir iletişim ağında kullanılması ile, havasal baz istasyonlarının iletişim ağı üzerinde olası etkileri artacaktır. En önemli problemlerden biri, havasal baz istasyonlarının uygun konumlara yerleştirilmesidir. Aksi takdirde, havasal baz istasyonlarının kapsama alanları, servis veren diğer karasal baz istasyonlarının kapsama alanları ile örtüşebilir. Böyle bir durumda, dayanıklı bir ağ elde edilmesi mümkün olmayacaktır. Özellikle, örtüşen bölgelerde bulunan son kullanıcıların hangi baz istasyonlarına tanımlanacağı ve örtüşmenin minimum düzeyde tutulacağı bir topoloji yönetimi tasarlamak oldukça önemlidir. Bunun yanında, havasal baz istasyonlarının yerleştirilmesi konusunda 3. boyutun da hesaplamalara dahil edilerek optimum yüksekliğin bulunması, dayanıklı bir ağ tasarımı için oldukça önemlidir. Dayanıklı bir ağ tasarımı için yukarıda bahsedilen problemlere ilave olarak havasal baz istasyonlarının enerji yönetiminin sağlanması, afet senaryolarının sürekliliği açısından önemlidir. Bir diğer önemli problem ise, aşırı yoğun ağlarda hizmet veren baz istasyonu sayısının fazlalığı ağın kapasitesini artırmaktadır. Bununla birlikte, baz istasyonu sayısının fazla olmasından dolayı hareketli kullanıcıların yol boyunca gerçekleştirecekleri geçiş sayısı da artmaktadır. Geçiş prosedürü kaynak ve hedef baz istasyonları arasında kontrol ve veri trafiğine ihtiyaç duymaktadır. Geçiş sıklığının artmasıyla kaynak ve hedef baz istasyonları arasındaki kontrol trafiği, kaynakların ve enerjinin daha fazla tüketilmesine neden olmaktadır. Aynı zamanda, hareketli kullanıcıların baz istasyonları arasındaki geçişlerde harcanan süreleri yani gecikmeleri artmaktadır ve bu durum kullanıcıların servis kalitesinde düşüslere neden olmaktadır. Sonuç olarak, yukarıda belirtilen ve günümüz iletişim ağları alt yapısı için tasarlanan 2 boyutlu algoritmalar ve yöntemler, topolojiye havasal baz istasyonu dahil edildiğinde devre dışı kalacaktır. Bunun en başta gelen nedenlerinden biri, havasal baz istasyonlarının, 3 boyutlu hareketliliği ve herhangi bir yol topolojisine sınırlı kalmadan hareket edebilme kabiliyetidir.

Bu tez çalışmasında, havasal baz istasyonlarının dayanıklı bir ağ tasarımında kullanılması durumunda, (i) havasal baz istasyonlarının konumlandırılması, (ii) enerji yönetimi, (iii) yol planlaması ve organizasyonu ile (iv) havasal baz istasyonları arasında gerçekleşebilecek handover (geçiş) prosedürünün yönetimi için, artan mobil veri trafiği ve dinamik topoloji değişikliklerine duyarlı, esnek ve merkezi bir yapı ile çözüm sunulmaktadır. Yazılım-tabanlı bir model ile kontrolör üzerinden havasal baz istasyonlarının yönetilmesi hedeflenmiştir. Bu kapsamda, karasal baz istasyonlarının servis dışı kaldığında bir kontrolör üzerinden gerçekleştirilecek fonksiyonlar ile havasal baz istasyonlarının güvenilir ve devamlı bir iletişim sağlaması için bir model önerilmiştir.

Tez çalışmasının ilk kısmında, verilen bir coğrafi alanda, ihtiyaç duyulacak minimum sayıda havasal baz istasyonu sayısını tanımlayarak, 3 boyutlu konumlandırma problemi ele alınmıştır. Önerilen konumlandırma algoritması ile havasal baz istasyonlarının kapsama alanları tanımlanmış ve enerji yönetimi ile havada kalma süreleri kontrol edilmiştir. Özellikle, havasal baz istasyonlarının sınırlı kapasitede bataryaları olduğu ve havasal ağlara yeni katılan ya da ağdan ayrılan havasal baz istasyonları için ağın yeniden organize olması gerektiği düşünüldüğünde, mevcut havasal baz istasyonlarından en etkin şekilde yararlanmak oldukça önemlidir. Bu maksatla son kullanıcılara kabul edilebilir bir servis kalitesinde hizmet vermeleri için

havasal baz istasyonlarının enerji yönetim mekanizmaları ile yeniden şarj edilebilmesi için ikmal istasyonlarının etkin yönetimi üzerinde bir model önerilmiştir.

Havasal baz istasyonlarının değişken ve olası bağlantı kesintileri, kaynak tahsisi ve kanal planlamasında problemlere neden olmaktadır. Bu maksatla, havasal baz istasyonlarının yönetimi için ağ fonksiyonlarını yönetmek ve kritik zamanlarda, bu problemlere yönelik çözümler sunmak gerekmektedir. Özellikle, havasal baz istasyonlarında gerçek zamanlı izleme, uyarı tetikleme gibi kritik ortamlarda veri aktarımında meydana gelebilecek bir gecikme ağ fonksiyonlarının merkezi yönetimi ile gerçekleştirilebilir. Bu maksatla, tez çalışmasının son kısmında ise, havasal baz istasyonları arasında gerçekleşebilecek geçiş prosedürünün yönetimi için bir ağ mimarisinin gerçekleştirilmesi hedeflenmiştir.

Karasal baz istasyonları için belirtilen geçişe bağlı problemler, havasal baz istasyonu kullanıldığında da geçerliliğini korumaktadır. Ek olarak, bu problem havasal baz istasyonlarının zaten kısıtlı olan kaynaklarını ve enerjilerini daha hızlı tüketmesine neden olmaktadır. Bu problemin çözümünde geçiş sıklığının ve dolayısıyla havasal baz istasyonlarının kullanıcı başına harcadığı enerjinin azaltılması için yazılım tabanlı ağ mimarisinde bir geçiş karar verme ve geçiş gerçekleştirme mekanizmaları önerilmektedir. Böylece dinamik ağ topolojilerine duyarlı, havasal baz istasyonları ile desteklenebilen ve havasal baz istasyonlarının kullanımından kaynaklanan problemleri minimize eden merkezi ve esnek bir yaklaşım önerilmiştir.



1. INTRODUCTION

Resilience is the ability of a system to deal with faults, changes or challenges. Resilience is used in many disciplines including ecology, psychology, economy and community. It is defined as "The persistence of relationships within a system; a measure of the ability of systems to absorb changes of state variables, driving variables, and parameters, and still persist" in ecological system [2]. It is defined as "A sustainable network of physical systems and human communities, capable of managing extreme events; during disaster, both must be able to survive and function under extreme stress" in community [3].

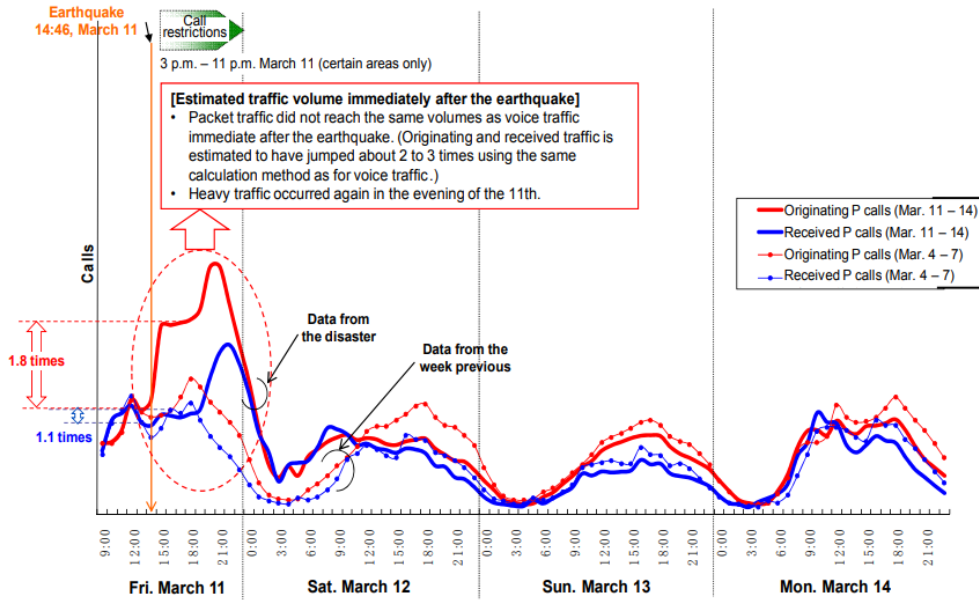
The emergence of resilience systems in communication networks provides an acceptable level of service in the face of faults and challenges to normal operation [4] and it has potential to completely reshape the traditional networks. Resilient networks have emerged to manage the risk of disaster-based cascading failures associated with complex interdependent systems.

In particular, flood, hurricane, earthquake and other natural hazards can not be prevented. Because of the climate changes, some risks will grow. Increased flooding, frequent and more intense extreme weather events threat the communities. After the hazard has passed, it is important to recover efficiently within a reasonable time for communities. Therefore, communication networks should be protected against natural disasters, (e.g. earthquake, hurricane, flood) or malicious attacks (e.g. cyber attacks) since such disruptions of critical infrastructure threaten the security, economy, and public safety. It is necessary to enhance resilience of the critical infrastructure that encourages efficiency, innovation, and economic prosperity.

In the aftermath of a large scale natural disaster, communication infrastructure plays an important role. Unfortunately, the current network infrastructure is static and non-adaptive which makes it nearly impossible or consumes a lot of time to reconfigure the network to react a disaster-based failures. Resilience and robustness are key issues to guarantee a high network availability and reliability. Two failure scenarios can be

considered: (i) localized malfunction (e.g. failure in one equipment) (ii) large-scale damages due to the natural disaster.

In case of the failure of Base Stations (BSs), it is tremendously time-consuming to redesign the network. For example, after 2011 Tohoku Earthquake in Japan, most of the BSs became out-of-service and the Internet had become available barely after 7 days. 12 communication buildings demolished and 16 of them flooded [5]. In addition, during natural disasters, packet traffic can unexpectedly increase. In Tohoku Earthquake, packet traffic is calculated 1.8 times higher than the normal periods [1] as seen in Figure 1.1. Reactivation of inaccessible BSs makes the topology control and connectivity a challenging task. Therefore, existing network infrastructure needs some mechanisms to reduce possible effects after such unexpected environments.



Natural disasters could potentially cause disruptions to communications and information technology. Lack of communication systems during and immediately after a natural disaster increases the impacts of the disaster. Effective communications should be maintained for the rescue operations and to help the affected communities. Since the terrestrial infrastructures may be damaged partially or totally in the disaster area, the use of aerial vehicles contributes to planning and designing alternative communication networks.

Recently, Aerial Base Stations (ABSs) represent one of the key capabilities for post-disaster communication due to autonomous driving, remote control, and providing continuous coverage of the target area. In case of malfunction of terrestrial BSs for example, in the event of a natural disaster, ABSs are useful to serve users and handle increasing traffic for specific periods. Accordingly, ABSs can be deployed and moved based on the user density and changes in traffic demands.

We use the programmability of Software-Defined Networking (SDN) to provide an acceptable level of service against faults, changes or challenges [4]. SDN offers several novel features that can address the challenges in Chapter 1. The separation of control and data planes allows us to utilize the available network information [6]. To manage the ABSs in a coordinated manner, the information gathered at the control plane enables the centralized decision making.

ABS deployment assists terrestrial networks to minimize the disruptions caused by unexpected and temporary situations. However, because of the physical limitations with low-capacity power supplies; they have limited flying time, limited velocity and communication range. According to Study on Enhanced Long Term Evolution (LTE) Support for Aerial Vehicles [7], the Reference Signal Receive Power (RSRP) and Received Signal Strength Indicator (RSSI) characteristics of aerial vehicles are different from the terrestrial BSs. Due to their high line-of-sight propagation probability, ABSs experience increased interference and channel fluctuation. ABSs have vertical movement and direction switching. This results in frequent service interruptions and a higher handover failure rate [8]. In addition, high number of ABSs and inappropriate 3D deployment within the target area may result in frequent and unnecessary handover. For all these reasons, there are various problems in the system design while trying to accomplish real-world problems and complicated duties. Therefore, in order to increase resiliency in aerial networks, a proper positioning management, a flight planning mechanism and handover procedure are needed considering the relationship between ABS flight characteristics and energy consumption.

1.1 Purpose and Scope of the Thesis

According to the Weather, Climate & Catastrophe Insight 2017 Annual Report [9], the direct economic damage of weather and climate topped USD 353 billion in 2017. Thus, over the last years, interesting novel technologies have emerged for disaster assistance with the highly mobile and low-cost aerial platforms. The aim of such aerial platforms is to meet urgent communication needs in mission critical environments. Especially, the use of ABSs, e.g. drones, has become a prominent solution: when the existing terrestrial network is temporarily damaged, ABS-based wireless communications can provide adaptive coverage and high service quality for User Equipments (UEs) on the ground. In addition, it is expected that nearly 12% of global mobile traffic will be 5G cellular connectivity by 2022, where an average 5G connection will generate 21GB traffic per month [10]. Thus, the use of ABSs also assists to increase the coverage of the existing terrestrial networks.

It can be seen that it is infeasible and impractical to design and deploy hardened structures, equipment, and transmission facilities that never fail and can withstand any disaster. Therefore, the main objective of this thesis is to propose a mechanism that the network will be resilient with an acceptable level of performance and recover from the disaster.

The ABS connectivity is built on top of the existing terrestrial wireless networks. Compared to conventional BSs, ABSs can adjust their positions and provide on-demand communications. However, due to the weight and size constraints, ABSs have limited operational time before the batteries are recharged. Their limited battery capacities affect the network lifetime sacrificing throughput. Although multiple ABSs ensure high service quality to the UEs, they introduce several algorithmic challenges, specifically in terms of energy-aware optimal deployment, flight endurance, scheduling the ABSs' operations and handover procedure. The success of this technology rests on (i) energy efficient deployment and (ii) controlling ABSs' operations in a coordinated manner. Defining the ABS positions is an important first step in network planning for long-lived aerial networks. Then, energy saving mechanisms and intelligent duty cycle can be managed by a control station.

In this thesis, we focus on a practical scenario, where ABSs provide emergency coverage to the disaster area after failures of terrestrial BSs as shown in Figure 1.2. We provide a continuous coverage model that aims to maximize hover time through an energy efficient deployment and reduces battery recharging time. The control station implements *optimal ABS deployment, maximizing endurance, path planning, scheduling for recharging and handover mechanism* functionalities to manage ABSs. The control station identifies the optimal subset of UEs, via a deployment algorithm, to assign ABSs. After the placement of ABSs, the control station now tracks the consumed energy to specify the time for which ABSs should be recharged. Thus, the key challenges in creating such a model are: (i) ensuring a coverage model for ABSs from an online perspective, (ii) maximizing the flight endurance to serve UEs as long as possible, and (iii) scheduling the operations of ABSs. Note that user demands can vary over time in unpredictable ways and satisfying these demands requires flexibility to reconfigure the network in an online manner. Thus, this thesis explores a scenario where user demands are not entirely predictable and not known a priori.

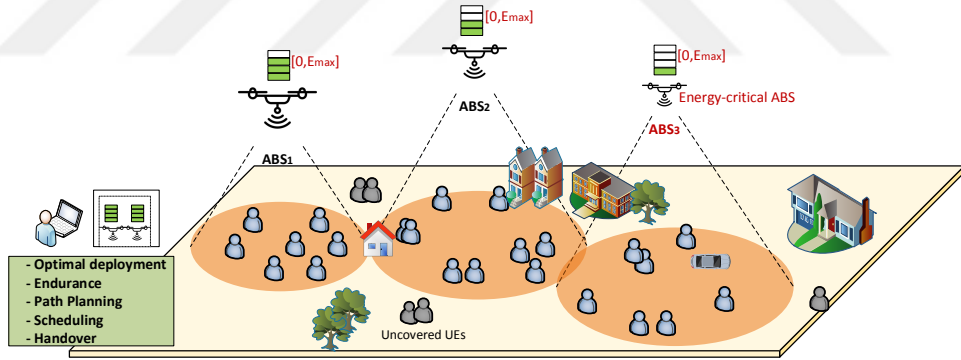


Figure 1.2 : Considered scenario for aerial networks.

We also explore a reinforcement based Q-learning framework for energy-aware ABS deployment, which is an effective method, where the environment is unknown. The main problem in aerial networks is to maintain continuous service to the users considering ABS battery recharging or replacing interruptions. This triggers an increase in the handover delay and handover failure ratio. Thus, we investigate the handover procedure for aerial networks. Since the handover procedure is different from traditional handover procedure, we propose a solution that does not require extended message complexity considering 3D coordinates of each component in the network.

1.2 Thesis Overview

This thesis presents an energy efficient software-based solution for ABSs, referred to as *AirNet* and which improves user coverage and flight endurance, and reduces handover failure ratio. This thesis is structured as follows:

- **Chapter 2** gives an overview of the state-of-the-art systems, frameworks and models in aerial networks.
- **Chapter 3** describes the design and implementation of the network architecture.
- **Chapter 4** describes the proposed system model, named as *AirNet*, that provides an energy-aware solution to deploy and schedule the ABSs and maximize the hover time with an endurance framework. This also gives the handover procedure for aerial networks. An optimal placement algorithm is proposed to maximize the covered UEs under the limited battery capacity and limited number of ABSs. The demand-aware configuration is also analyzed from an online-manner perspective in Chapter 4.1, Chapter 4.2 and Chapter 4.3. We use an energy model to improve the flight endurance and derive an efficient recharging strategy such that the total energy consumption of all ABSs is minimized. We also consider the affecting parameters including weight, flying time and flying speed. A path planning strategy is presented to provide less energy consumption and less computational complexity in Chapter 4.4. A scheduling mechanism is provided to assign ABSs to the limited number of replenishment stations, which can avoid the ABSs from being out of service for a long time in Chapter 4.5. A handover decision algorithm is proposed to minimize the computational complexity of ABSs. Then, handover execution steps are presented to serve UEs continuously in Chapter 4.6.
- **Chapter 5** evaluates the proposed model introduced in Chapter 4.
- **Chapter 6** concludes the thesis by summarising the work and results and providing some directions for future work.

2. LITERATURE REVIEW

When a natural disaster occurs, coordination of disaster management operations is of vital importance. More importantly, the operations must be done quickly and effectively to assist people, reduce the number of victims. ABSs can effectively assist in improving the situational awareness and assessment. They can monitor disaster area and collect the information to transfer ground control stations by taking photo/video record.

In this chapter, we will review the related works on resilience, energy-efficient deployment, maximization of flight endurance, path planning and handover management. We review the most related studies in these areas and discuss the novelty of our contributions.

2.1 Resilience in Communication Networks

Resilience is a new concept for many governments and agencies. There is a need to consider some risks against natural disasters, malicious attacks or faults so that some precautions can be taken into account to minimize its affects and adapt the changes. In communication systems, one of the main concern is how a system can be designed or redesigned to build resilient and reliable communication for individuals or groups [11]. Emergency communications should be resilient for a robust and continuous transmission. Therefore, it is important to describe and plan the management of communication in crisis situations.

In [12], the authors describe a number of resilience principles named as $D^2R^2 + DR$: Defend, Detect, Remediate, Recover, and Diagnose and Refine. The strategy defines the real-time control for dynamic changes and non-real time control to improve the design of network. Based on the real-time control, a resilient control model is developed. [13] presents a preventive protection model to increase network robustness and reduce the number of disconnections so that the authors provide insights for network operators to decide how to adjust threshold parameters in large-scale failure

scenarios. When the thresholds are defined, traffic flows that must be rerouted so that controller can change the routing table entries. [14] investigates resilience differentiation since resilience requirements may vary from application to application and it also depends on how the user applies the service. In addition, recovery procedures are classified to react to the failure, redirect the traffic and make the network more resilient. Fault management procedure is defined in terms of fault detection, fault localization, fault notification and recovery switching.

There is a high potential for UAVs in various sectors, including commercial and government services, especially search and rescue operations. Today, UAVs are in the foreground for high-risk life-threatening operations such as flying over a volcano or above a radiation-contaminated region [15]. UAVs are free to move in 3D space without restriction to road topology. This brings some flexibility in the emergency situations.

When a disaster occurs and normal communication breaks down, the lack of information flow could be vital importance in emergency situations. In this respect, CLOSE SEARCH [16] integrates in a small unmanned helicopter, a thermal sensor and a multi-sensor GPS-based navigation system with an Autonomous Integrity Monitoring capability, to support the search components of search-and-rescue operations, and to reach difficult-to-access areas and/or in time critical situations. RESCUECELL [17] aims at developing a cost-effective, robust and lightweight technology, that can easily be transported to the affected zone, and that allows spreading the nodes covering the entire zone, leading to the location of possible injured people swiftly within some minutes. SHERPA [18] develops a mixed ground and aerial robotic platform to support search and rescue activities in a real-world environment like the alpine scenario. ResiliNets [19] aims to understand and improve the resilience and survivability of computer networks, including the Internet. RESIST [20] targets reliability aware design methods and run-time adaptive approaches for next generation resilient integrated electronic systems in Automotive and Avionics. [21] considers time critical disaster situations and aims to rapidly acquire aerial imagery in dangerous terrains from different vantage points.

2.2 Coverage Problem and ABS Deployment

Most of the existing studies on aerial networks investigate how to maximize the number of covered users and optimal deployment. However, in addition to ABS deployment, it is also important to navigate an ABS to minimize energy consumption and schedule the ABSs' operations. Thus, it remains a question how it is possible to increase the network resiliency and manage ABSs' operations in mission critical environments.

In [22], the authors address multiple cooperative coverage problem for more reliable and efficient aerial scenarios and propose multi-UAV coverage model based on the energy-efficient communication. First, the coverage probability from a given UAV is derived. Then, transmission power is determined to maximize coverage utility. Although the locations of users are known a priori, the user demands cannot be entirely predictable and this affects the coverage model. In [23], the authors focus on maximizing the coverage area of a single ABS under the constraint of transmission power. Then, the relationship between antenna gain and antenna beam angle is set up so that the flight altitude and coverage radius are adjusted according to beam angle. However, the provided solution cannot be optimal with multiple ABSs. In [24], the authors propose a deployment algorithm for UAV-BSs that maximizes the number of covered users with the minimum transmission power. In the horizontal dimension, the deployment problem is modeled as a circle placement problem and the results are confirmed with different user heterogeneity. However, the proposed solution is designed for 2D space. In [25], analysis and optimization of air-to-ground systems are researched. The authors derive optimal UAV altitude for reliable communication and maximum coverage area. However, energy is also an important factor that needs to be included into the working system for reliable communication in aerial networks.

2.3 Maximizing Flight Endurance

Due to the battery constraints of ABSs, many research projects aim to minimize the duration of ABSs in reaching their designated locations so that hover time is maximized to achieve the assigned tasks. In [26], the authors deal with the deployment problem to transport UAVs in the shortest time. In addition, the computational

complexity is analyzed and an optimal solution is proposed. However, this problem is simplified by focusing on predetermined clusters so that coverage area adjustment is not considered. In [27], survivability of the battery-operated aerial-terrestrial communication links is investigated to improve energy efficiency. However, aerial networks are constructed into the center of the target area, but this cannot be practical to maximize coverage area. In [28], throughput coverage is investigated by optimally placing UAVs for public safety communication after a natural disaster. In contrast, the consumed energy of ABSs in our work is investigated and endurance is improved. In [29], flight time constraints of ABSs and the relationship between the hover time of ABSs and bandwidth efficiency are investigated. First, given the maximum possible hover time, average data service is maximized. Then, given the load requirements of users, average hover time of ABSs is minimized to serve the users. The key difference between [29] and our work is that we schedule the operations of ABSs to improve the flight duration and serve the users as long as possible. In addition, we also jointly consider transition and hover time, both of which contribute to maximize endurance.

2.4 Path planning

The feasibility of the path planning algorithms is related to shortest path problem to minimize the energy consumption. In addition, a safe path is constructed to arrive at the given target point since multiple ABSs can increase the collision probability. [30] uses aerial vehicles for disaster management with the aim of autonomous inspection. Then, the authors propose an energy-efficient path planning algorithm for flying, hovering and data transmission. [31] investigates path planning problem in 2D space in order to maximize the communication quality and guarantee higher throughput. To achieve these, the authors propose two path planning algorithms considering available energy and wind effect. [32] aims to optimize the location planning of ABSs considering Line of Sight (LoS) and Non-Line of Sight (NLoS) effect and uses Q-Network algorithm to solve the 3D placement problem. In our method, the controller monitors the traffic across the network and has complete knowledge about the topology and thereby, ABS only follows the defined tasks by the controller. This means that all decisions are intelligently given by the controller providing less energy consumption and less computational complexity. This thesis explores and analyzes a dynamic path planning

strategy that satisfies the constraints of ABSs' battery capacity. Furthermore, an optimized path guarantees the successful completion of the defined tasks with the minimum consumed energy.

Path planning also provides some mechanisms to guarantee safe navigation of drones while avoiding collisions. In particular, with the usage area of drones in a wide range of applications, e.g., search and rescue operations, packet delivery service, traffic monitoring, drones can only achieve their missions by continuously updating the target region [33]. In order to maximize the collected data and reach the destination, path planning algorithms determine a path between source and destination node pairs. These algorithms include genetic algorithms [34], particle swarm optimization [35] or building a probability map [36] etc. The transition to the designated locations may face several uncertainties according to different path planning algorithms, such as obstacles, high computational complexity and unpredictability.

In terms of the underlying algorithmic problems, the coverage problem in aerial networks is related to problems such as the set cover and sweep coverage problems. For example, the *Set Cover Problem* looks for the fewest sets to cover a given set of points in the plane, which is NP-hard [37]. Our optimization problem can be seen as a geometric version, where the set size also depends on the height of the ABS [38]. Another related optimization problem considers a scenario, where a mobile drone/autonomous robot can continuously move to collect data from targets. By doing this, the robots aim to minimize so called sweep period for the given targets or reduce the trajectory length. This problem is referred to as the *Sweep Coverage Problem* [39]. In both problems, the objective is to improve coverage utility and flight endurance by maximizing the energy efficiency. Following a similar objective, but considering a more general model, in this thesis, we study the control of ABSs' operations with a centralized controller and find an energy-aware 3D deployment for ABSs to maximize flight endurance. Consequently, we provide useful guidelines to control ABSs' operations.

2.5 Handover Management

Recently, many approaches have been proposed to cope with the handover problem for cellular networks. However, in aerial networks, the problem can be evaluated

differently from 2D solutions due to the mobile BSs. The efficiency of handover algorithms is a significant issue for providing better Quality of Service (QoS) to mobile users. For instance, [40] develops an analytical model for the handover rate in K-tier heterogeneous cellular networks. The relationship between horizontal/vertical handover rate and total handover rate is analyzed. [41] derives a mathematical formulation of the dynamic boundary area size by considering the user's mobility and signaling delay to define the handover initiation time. Similarly, [42]- [43] investigate the design of a handover management strategy and analyze the handover performance. While these works are useful for designing and optimizing terrestrial networks, they are not directly applicable to aerial networks due to the mobility of ABSs.

Because of the battery constraints of ABSs, handover is frequently required. Several studies are available in the literature, which analyze the performance of the handover procedure in aerial networks. However, some issues still remain. Especially, it is neglected that frequent handover decision and execution cause more computation at the ABSs and result in more energy consumption. In [44], the authors present a coverage decision algorithm by calculating handover success probability and false handover initiation probability. Received Signal Strength is used for the coverage decision algorithm. Similarly, [45] provides handover probability and the relationships with respect to the user velocity, altitude, and density of aerial vehicles. [46] proposes a handover control mechanism by predicting the user trajectories. Then, the authors present a handover decision method based on the users' received power. [47] proposes a method to transmit measurement signals for a stable handover of aerial vehicles. Furthermore, [48] analyzes the user and BSs antenna heights and studies inter/intra tier handover rates using tools from stochastic geometry. [49] proposes an efficient management and fast handover mechanism to decrease the handover latency, end-to-end delay, and signaling overheads. [50] considers two different scenarios for the speed of ABSs. Accordingly, ABSs move at the same speed or at different speeds. Then, the authors analyze the handover probability. [8] presents a mobility management model for a cellular network that supports drone communication. The proposed handover decision algorithm instructs the BSs to trigger the handover procedure. This enables to minimize handover failure ratio.

3. NETWORK ARCHITECTURE AND MODEL

LTE networks consist of two main components: (i) Radio Access Network (RAN) that provides connectivity between BSs and UEs, and (ii) Evolved Packet Core (EPC) that is responsible for mobility, management and control functions. In [51], an EPC design, named as SkyCore is proposed and emphasized that all distributed functionalities into a single logical entity can reduce control signal and latency so that UEs can access quickly. With this idea, we investigate the aerial networks and propose a software-defined solution that embedded into a controller to provide less computational complexity.

SDN-based network architecture is considered with a centralized controller that directs traffic according to user demands, thereby minimizing the computational complexity by individual ABSs. SDN architecture provides flexible ABS deployment and path planning and gives the handover decision for less energy consumption. This simplifies the network management since ABSs are directly programmable and abstracted to the data plane. As a first step, this work aims to maximize the number of covered users to meet stringent QoE requirements and assign appropriate number of UEs to the ABSs. Then, it minimizes the energy consumption for path planning. Finally, a handover decision algorithm is proposed to minimize the computational complexity of ABSs under the limited battery capacity.

This thesis introduces to an existing SDN-based network, few key components given in Figure 3.1. (1) *Controller* is responsible to collect data from the data plane including UE locations and traffic demands. Then, the controller sends the flight control information to the ABSs executing the main operations. (It will be explained in Chapter 4). A graph model is also constructed to make a strategy for *path planning*. (2) *ABSs* are managed on-the-fly by the controller and ensures continued and reliable services for all attached UEs. ABSs are triggered by the controller at the battery recharging time.

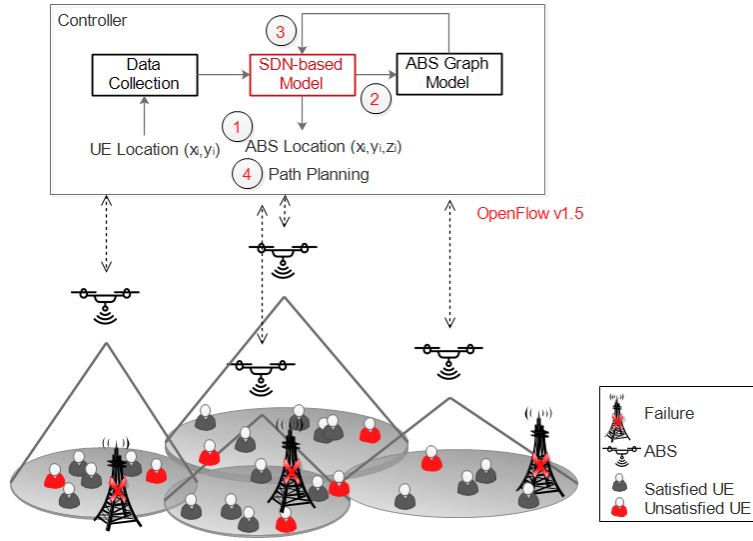


Figure 3.1 : Considered scenario for SDN-based aerial networks.

Each ABS includes Global Positioning System (GPS), Radio Access Technologies (RATs) such as LTE, and network equipment which is controlled with a remote centralized controller via OpenFlow v1.5 southbound application program interfaces (APIs). SDN southbound APIs are used to communicate between ABS and controller through a dedicated controller channel. ABSs provide operational information such as position, battery levels, route to the controller. UEs' information is also collected by the SDN controller including position and traffic demand. Then, SDN controller calculates and implements the proposed solution.

The controller has direct access to data plane via *OpenFlow v1.5* protocol. Flow table in *OpenFlow v1.5* protocol is reorganized for adaptive and globally optimized flow management as shown in Figure 3.2. The flow table consists of match fields that describe the special handling between the controller and ABSs. We redefine the message format on conventional *OpenFlow match fields*. This field is divided into 4 parts including ABS id, position, UE id and priority for the communication from control plane to data plane. Similarly, for the communication from data plane to control plane, the field is divided into three parts including UE id, position and traffic request. In order to manage ABSs, the controller collects the information from the data plane and then manages to ABSs with the proposed model.

After the connection establishment between ABS and UE, one traffic stream is supplied and traffic is added to the topology over time. To give an exemplary illustration, ABSs are located to the different altitudes and one ABS is used to cover maximum 4 UEs

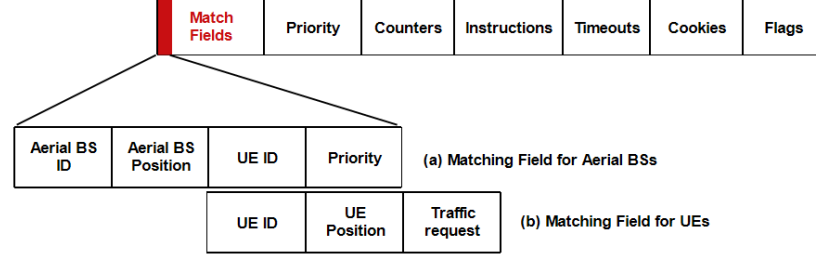


Figure 3.2 : OpenFlow table message format.

as shown in Figure 3.3. When the simulation time passes, UEs are connected to the ABSs and medium is occupied. For a given ABS_1 (red lines) and ABS_2 (black lines), full lines indicate the altitude during serving UEs. Update rates are 10 times per second to aggregate the current state in the data plane, such as position, traffic demand. The connection starts when medium is free. For example, UE_1 and UE_2 occupied the medium at the same time. Then, UE_2 released the connection, but UE_1 still continue the connection with ABS_1 .

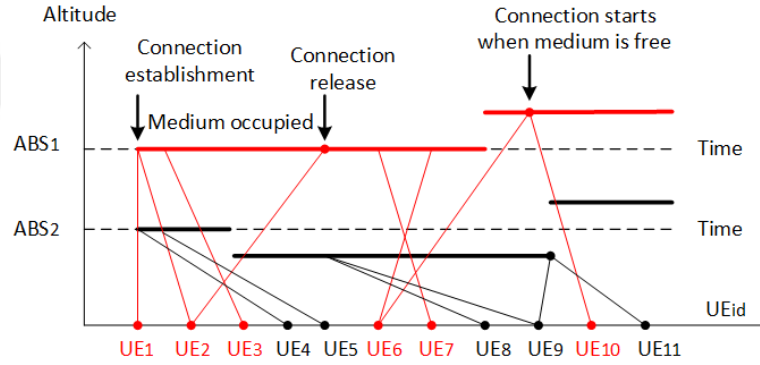


Figure 3.3 : Connection between ABSs and UEs.

3.1 Network Model

We consider a square area of size Am^2 ($a(m) \times a(m)$) with M number of ABSs to cover the target area. Each ABS serves the UEs, where UEs are uniformly distributed to the target area. An ABS recharges its battery at the replenishment station which is located on a mobile station. Each ABS can be in one of the following states. An ABS life cycle is shown in Figure 3.4.

- Transiting State (s_{trans}): After the determination of the ABS locations, the consumed energy from the initial location to the designated location and also from

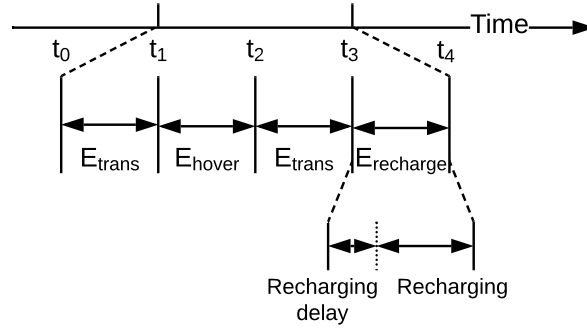


Figure 3.4 : ABS life cycle.

the designated location to the initial location are followed in this state. We refer to the transition times as $t_1 - t_0$ and $t_3 - t_2$, respectively.

- **Hovering State (s_{hover}):** In this state, UEs remain connected with ABSs and get service. We denote the hover time as $t_2 - t_1$.
- **Recharging State ($s_{recharge}$):** The ABS is on the replenishment station to recharge its battery.
- **Sleeping State (s_{sleep}):** If all replenishment stations are used by other ABSs and there is no available station for recharging, the ABS waits in this state. In addition, if no task is assigned to the ABS by the control station, the ABS is in this state until a new task is assigned.

In addition, we assume that each ABS starts with a maximum and identical energy capacity, equal to E_{max} . The consumed energy from initial location $(0,0,0)$ to the designated location (x_j, y_j, z_j) (transiting state) will directly affect the lifetime of the ABS since the coverage utility depends on the available energy at the ABS.

The mean value of the interference between ABSs, the coverage probability of the UE_{*i*} is [52]:

$$\begin{aligned}
 P_{cov,i} &= \mathbb{P}\left[\frac{P_{r,i}}{N+I} \geq P_{threshold}\right] \\
 &= P(LoS)_i \mathbb{P}[P_{r,i}(LoS) \geq P_{min}] + P(NLoS)_i \mathbb{P}[P_{r,i}(NLoS) \geq P_{min}] \quad (3.1)
 \end{aligned}$$

where P_{min} is the minimum received power, $P_{min} = 10\log(NP_{threshold} + IP_{threshold})$, N is the noise power. We assume that noise power does not change over time for all receivers for simplicity and is equal to $-120dBm$. $P_{threshold}$ is the Signal-to-Interference and Noise (SINR) threshold ratio. This shows the necessary

condition for connecting the UEs to ABS and I is the interference power received from the nearest ABS_k [52]:

$$I \approx P_t g(\varphi_k) \left[10^{\frac{-\mu_{LoS}}{10}} P_{LoS,k} + 10^{\frac{-\mu_{NLoS}}{10}} P_{NLoS,k} \right] \left(\frac{4\pi f_c d_k}{c} \right)^{-n} \quad (3.2)$$

where P_t is the transmission power of ABS, $g(\varphi_k)$ is antenna gain and $g(\varphi_k) \approx 29000/\theta^2$ [52], θ is elevation angle, f_c is the carrier frequency, c is the speed of light. μ_{LoS} and μ_{NLoS} are the mean of the shadow fading for LoS and $NLoS$ and n is the path loss exponent ($n = 2$).

The received signal from ABS for UE_i is as follows [53]- [54]:

$$P_{r,i}(dB) = \begin{cases} P_t + g - PL_{LoS,i} - \chi_{LoS}, & \text{for } LoS \text{ link} \\ P_t + g - PL_{NLoS,i} - \chi_{NLoS}, & \text{for } NLoS \text{ link} \end{cases} \quad (3.3)$$

where $\chi_{LoS} \sim N(\mu_{LoS}, \sigma_{LoS}^2)$ and $\chi_{NLoS} \sim N(\mu_{NLoS}, \sigma_{NLoS}^2)$ are the impact of shadowing caused by obstacles with normal distribution. $(\mu_{LoS}, \sigma_{LoS}^2)$ and $(\mu_{NLoS}, \sigma_{NLoS}^2)$ are mean and variance of shadow fading for LoS and $NLoS$ where $\sigma_{LoS}(\theta_j) = k_1 \exp(-k_2 \theta_j)$ and $\sigma_{NLoS}(\theta_j) = g_1 \exp(-g_2 \theta_j)$, respectively [52], [55]. The values of k_1, k_2, g_1, g_2 depend on the environment and they are constant. PL_i is the path loss. We use the path loss model for air-to-ground communication over urban environments. Each UE will have a LoS and $NLoS$ links with some probabilities by connecting to the ABS. This probabilities depend on the location of UE and ABS, and environment. The LoS probability between the ABS and UE is given by [53], [54]:

$$P(LoS)_i = \frac{1}{1 + a \cdot \exp(-b[\theta - a])} \quad (3.4)$$

where a and b are constant values that depend on the type of the environment (rural, urban etc). θ is the elevation angle and equal to $\theta = \frac{180}{\pi} \arctan(\frac{h}{d_i})$. h and d_i represent the altitude of the ABS and distance between the ABS and UE_i . Note that the $NLoS$ probability between UE and ABS is equal to $P(NLoS)_i = 1 - P(LoS)_i$.

Then, the path loss model for LoS and $NLoS$ is given by [53]- [54]:

$$PL_i(dB) = \begin{cases} 20 \log \left(\frac{4\pi f_c d_i}{c} \right) + \eta_{LoS}, & \text{for } LoS \text{ link} \\ 20 \log \left(\frac{4\pi f_c d_i}{c} \right) + \eta_{NLoS}, & \text{for } NLoS \text{ link} \end{cases} \quad (3.5)$$

where η_{LoS} and η_{NLoS} are additional path loss coefficients and equal to 1 and 20, respectively for urban environments [55].

3.2 Architectural Model

Figure 3.5 shows the implementation of the control architecture. The control station executes the proposed model, *AirNet*. A *task* is defined for each ABS by the control station. An ABS is equipped with an RF receiver to receive control signals sent by the control station. ABS initially follows its fixed task and no external communication is required. However, the defined task can be updated by the control station based on the network architecture. The *set up* block provides flight control information including hover location, coverage area, flight route and speed. The *critical controller* only includes the critical control functionality to provide an indication for energy consumption. In every time unit, control decisions are computed by the control station, and commands are sent to the ABSs. Once the consumed energy is known, the remaining energy information is evaluated based on the distance between the replenishment station and ABS so that timely and adaptive control decisions work in software. For this purpose, the *dynamics* block stabilizes the ABS. Rather than periodically triggering the controller of ABSs, we only run the set up block when an update is needed and the critical control is checked when the critical energy threshold is reached.

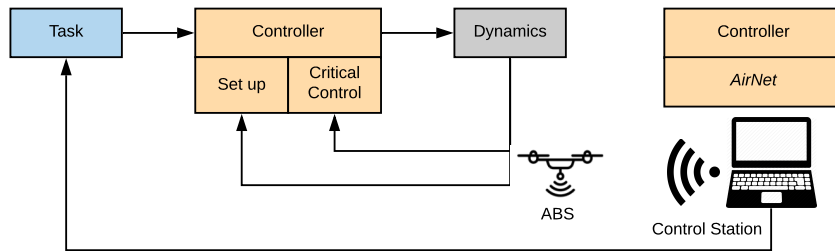


Figure 3.5 : Control architecture.

4. *AirNet* SYSTEM

The proposed system model, named as *AirNet*, provides an energy-aware solution, to deploy and schedule the ABSs and maximize the hover time with an endurance framework. This also provides the handover procedure for aerial networks. A general flow chart is shown in Figure 4.1. As seen in the figure, we determine the locations of ABSs in Algorithm 1. After ABS deployment, we calculate the consumed and residual energy, and update the location of the mobile control station in Algorithm 2. In order to maximize flight endurance, we propose Algorithm 3. After the ABS's battery is at a critical level, we propose a path planning strategy in Algorithm 4 and schedule the ABS operations for recharging in Algorithm 5. We will describe *AirNet* in multiple steps.

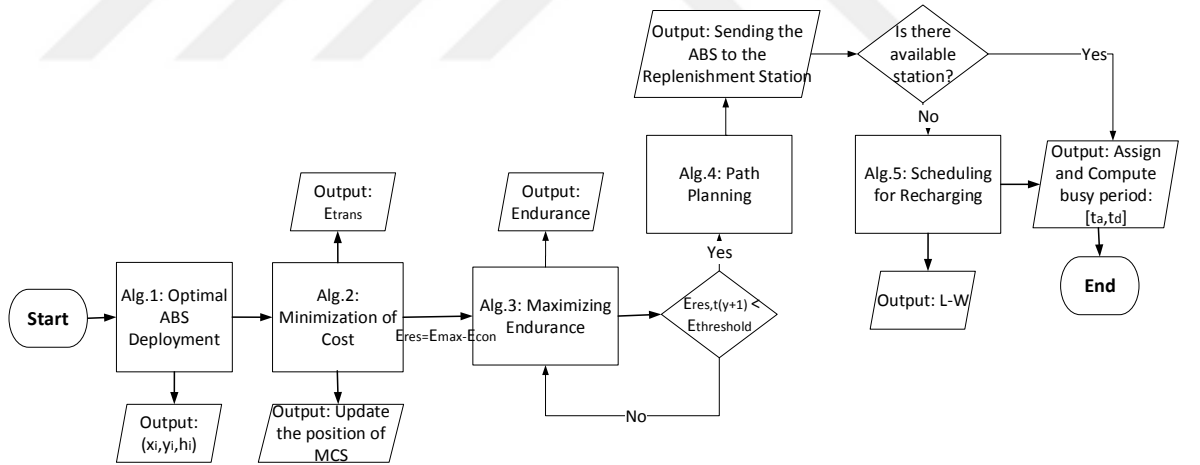


Figure 4.1 : *AirNet* flow chart.

4.1 Optimal ABS Deployment

We first focus on a single ABS deployment to cover the target area. To simplify the presentation, as shown in Fig. 4.2, the target area is divided into grid cells. Here, the number of UEs can vary from cell to cell. Our main idea for this demonstration is to observe the density of the UEs in the target area. If a cell includes a number of UEs, the cell is marked as '1'. Otherwise, it is marked as '0' to show the empty cell. This means

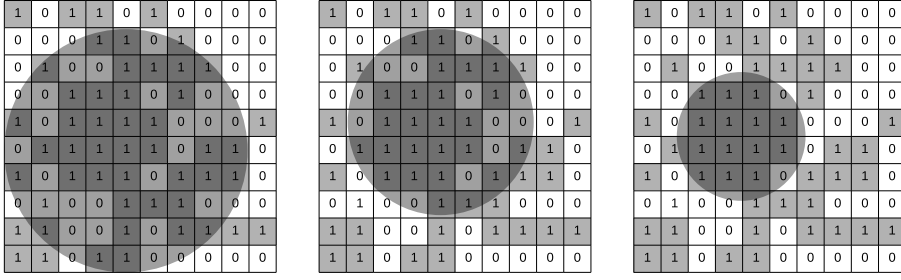


Figure 4.2 : Adjustment of coverage area with a single ABS.

that there is no UE in this cell. Depending on the altitude of the ABS, the coverage area also changes. Here, we define $R_{cluster}$ so that UE can only be connected to the ABS in this cluster. At the initial phase, according to the UE locations, we find the center of minimum radius to cover maximum number of UEs. Mathematically, with the *Chebyshev Center* formulation, the problem can be written as follows:

$$\min_{\mathbf{x}, R_{cluster}} R_{cluster} \quad (4.1)$$

subject to

$$\|\mathbf{x} - UE_i\| \leq R_{cluster}, \quad i = 1, 2, \dots, U. \quad (4.2)$$

where \mathbf{x} is the center point of the cluster and U is the number of UEs. However, it may not be effective when the whole target area is only covered by a single ABS since each UE cannot have a good signal quality for a given transmission power and flight altitude. Therefore, we first define $R_{cluster}$ with h_{max} and then check the received power of the UEs with the SINR threshold value as given in equation 3.1. At each step, we repeat this process with $h^* = (h_{min} + h_{max})/2$ until the solution is feasible. Then, we update the coverage area radius with Algorithm 1 as shown in Figure 4.2. According to [56], the height of the small unmanned aircraft cannot be higher than 400 feet above ground level. Thus, under the SINR connection model, the altitude is adjusted between $h_{min} = 20m$ and $h_{max} = 100m$ to determine the strength of the received signal from the desired ABSs and avoid interference caused by other ABS and the noise power. Optimal ABS altitude enables maximum coverage area with a minimum required transmission power, where h_j^* represents optimal altitude and $h_{min} < h_j^* < h_{max}$ as shown in Fig. 4.3.

Algorithm 1 solves the deployment problem with the computational complexity of $O(n \log n)$. The analysis is performed for each ABS. We first note that h^* produced by

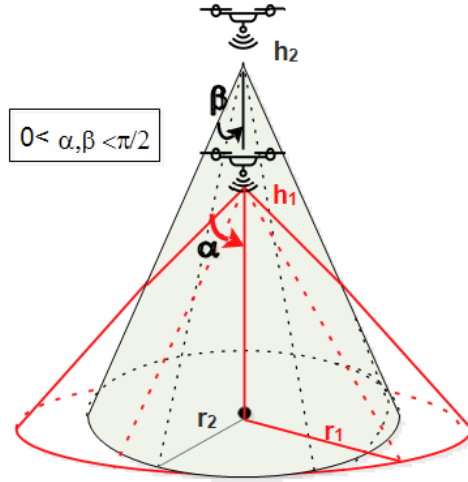


Figure 4.3 : Coverage area as result of different altitude of deployed ABSs.

Algorithm 1 is feasible. Otherwise, Algorithm 1 ends when $\left[\frac{P_{r,i}}{N+I} \geq P_{threshold} \right]$ for each $UE_i \in R_{cluster}$. Since we adjust the altitude between h_{min} and h_{max} for each ABS, we start with a maximum altitude to cover the UEs as much as possible. Suppose we have the solution $x = (x_1, x_2, \dots, x_m)$, $y = (y_1, y_2, \dots, y_m)$ with optimal altitude $h = (h_1, h_2, \dots, h_m)$. With the defined $R_{cluster}$ as given in equation 4.1, $Tolerance = \left[\frac{P_{r,i}}{N+I} \geq P_{threshold} \right]$ is checked for each $UE_i \in R_{j,cluster}$. This is repeated for each deployed ABS. Please note that ABSs are directed to the designated location along a flight path by minimizing the travel length.

Algorithm 1: Optimal ABS Deployment

Data: $h_{min} \leq h^*$, $h_{max} \geq h^*$

$Tolerance : \left[\frac{P_{r,i}}{N+I} \geq P_{threshold} \right]$

1 **repeat**

2 (1) $h^* = (h_{min} + h_{max})/2$
3 Solve the feasibility problem (1)
4 **if** (1) is feasible **then**
5 $h_{max} = h^*$
6 **end**
7 $h_{min} = h^*$

8 **until** $\forall UE_i \in R_{cluster} \left[\frac{P_{r,i}}{N+I} \geq P_{threshold} \right];$

With M ABSs and U UEs, the relationship can be represented as $a \in \mathbb{A}^{M \times U}$, where $a_{ij} = 1$ if UE_i is covered by ABS_j , otherwise $a_{ij} = 0$. Also we define a cost parameter, which is the consumed transition energy from the initial position to the designated

position for ABSs. The consumed transition energy is given in equation 4.3 [57]- [58]:

$$E_{trans} = \left(\frac{P_{full} - P_s}{v_{max}} v_d + P_s \right) (t_1 - t_0) \quad (4.3)$$

where v_d is the constant ABS speed during the trip, v_{max} is the maximum speed of the ABS and $t_1 - t_0 = d/v_d$, d is the flying distance with a constant velocity. P_{full} is the hardware power level when the ABS is moving at full speed and P_s is the power level when ABS stops in a fixed position ($v_d = 0$). The optimization problem aims to minimize the consumed transition energy from the deployed location to the initial location for the ABSs as given in equation 4.4.

$$\min \sum_{j=1}^M \left[\left(\frac{P_{full} - P_s}{v_{max}} v_d + P_s \right) \vartheta_j \right] (t_3 - t_2) \quad (4.4)$$

subject to

$$C_1 : \vartheta_j \in \{0, 1\} \quad j \in M \quad (4.5)$$

$$C_2 : \sum_{j=1}^M a_{ij} \vartheta_j \leq 1 \quad \text{for each UE} \quad (4.6)$$

where ϑ_j is a binary variable to follow active ABSs. C_2 indicates that a UE cannot get service from more than one ABS. $a_{ij} = 1$ if UE_i is covered by ABS_j , otherwise $a_{ij} = 0$. M is the number of ABSs. $(t_3 - t_2)$ is the transition time, where $t_3 - t_2 = d/v_d$, d is the flying distance with a constant velocity.

As seen in Fig. 4.4, the duty cycle of an ABS starts with the transition. The residual energy will decrease over time so that after ABS deployment, we focus on decreasing transition energy from designated location to the replenishment station as given in equation 4.4. To do this, we propose to update the location of the control station while guaranteeing the minimization of cost with Algorithm 2. Here, we also aim to cover a maximum number of UEs when the number of ABSs is limited. While the maximum coverage problem is NP-hard under the limited ABS (Line 2-5), we can obtain a greedy approximation factor of $1 - \frac{1}{e}$, which is explained in Appendix A [59].

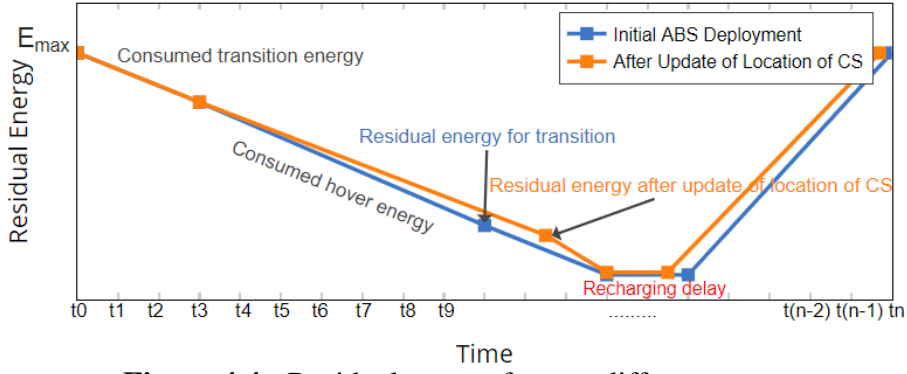


Figure 4.4 : Residual energy for two different cases.

Algorithm 2: Minimization of Cost

```

1 Initialize:  $E_{trans,j} \leftarrow \emptyset$  and  $U \leftarrow X$  ( $U$  is the set of uncovered UEs and  $X$  is the
  finite set of UEs)
2 while  $\forall ABS_j$  is deployed do
3   | Let  $S$  be a set such that  $|S \cap U|$  is maximized ( $S$  covers the largest number
  of UEs in  $U$ )
4   |  $U \leftarrow U \setminus S$  (remove from UEs in  $U$  that are covered by  $ABS_j$ )
5 end
6 DemandAwareReconfiguration() // cf Section 4.2
7 Update  $(x,y)$  position of MCS as  $(x,y) = \frac{S_{1,x,y}, \dots, S_{M,x,y}}{M}$  ( $S_{1,x,y}$  is the center point
  of set  $S_1$ )
8 for  $j \leftarrow 1$  to  $M$  do
9   | Calculate  $E_{trans,j}$  with equation 4.3
10 end
11 return  $E_{trans,j}$ 

```

While a detailed evaluation is given in Chapter 5, to get some intuition on the effectiveness of the algorithms, we first conduct simple experiments. This is performed in MATLAB for an environment with one and two ABSs, respectively. Then, the commands are tested with MAVProxy 1.5.0 that runs on Software In The Loop (SITL) ArduPilot simulator using Cygwin [60]. We observe the coverage areas for a better understanding of the network performance. Figure 4.5 shows the deployment of one ABS with $(10^{-4}UEs/m^2)$ and two ABSs with $(2 \times 10^{-4}UEs/m^2)$, respectively.

With different UE densities, we show the relationship between the coverage radius, $R_{cluster}$ and optimal altitude in Figure 4.6(a). After the optimal height is obtained, as the height of ABS increases, the coverage radius will decrease because of the SINR. We also illustrate the coverage ratio with the increasing number of ABSs for $(10^{-4}UEs/m^2)$ and $(2 \times 10^{-4}UEs/m^2)$ densities in Figure 4.6(b). Then, we compare two different scenarios in Figure 4.6(c) with 5 ABSs. At first, we deploy

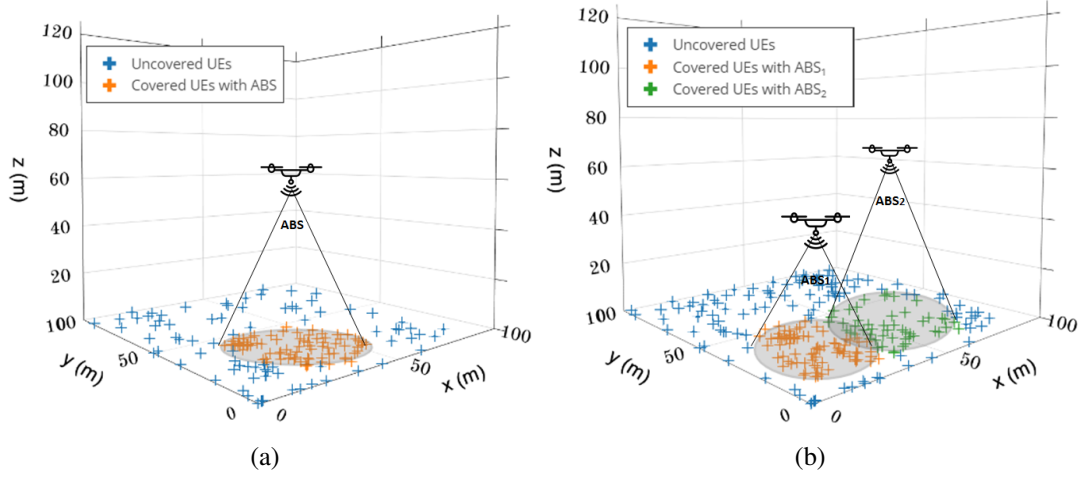


Figure 4.5 : (a) Coverage area with single ABS ($10^{-4} \text{UEs}/\text{m}^2$) (b) Coverage areas with 2 ABSs ($2 \times 10^{-4} \text{UEs}/\text{m}^2$).

ABSs and calculate the consumed transition and hover energy with Equations 4.3 and 4.16, respectively. Then, we update the location of control station as explained in Algorithm 2 and obtain average 14% degradation in terms of the consumed transition energy. This will increase the hover time of ABSs.

4.2 Demand-Aware Reconfiguration

The key feature in this approach is that *AirNet* supports demand-aware operation. User demand can vary over time in an unpredictable way, which leads us to analyze time-varying user demand. Satisfying the dynamic user demand requires reconfiguration in an online manner.

To achieve this, we check the traffic load of each ABS for the demand-aware reconfiguration. Here, we only focus on overlapping areas since coverage areas and the position of ABSs can be reconfigured to satisfy users' demands. Overlapping areas are the regions where UEs can connect k -ABS since this region is covered by k -ABS. Therefore, we assign the UEs in the overlapping areas to the ABS which has low traffic load.

Traffic demands are kept in a Demand Matrix, for each time t_y , where $t_1 < t_y < t_2$ and is represented as $|MxU|_{t_y}$. An entry $D_{(i,j)}$ in D is the demand from UE_i to ABS_j . It is assumed that the demands have variable packet size, L_i with power law distribution and their arrival rate, λ_i with Poisson distribution. Since user demand can vary with different types of applications, there should be a fair resource allocation among

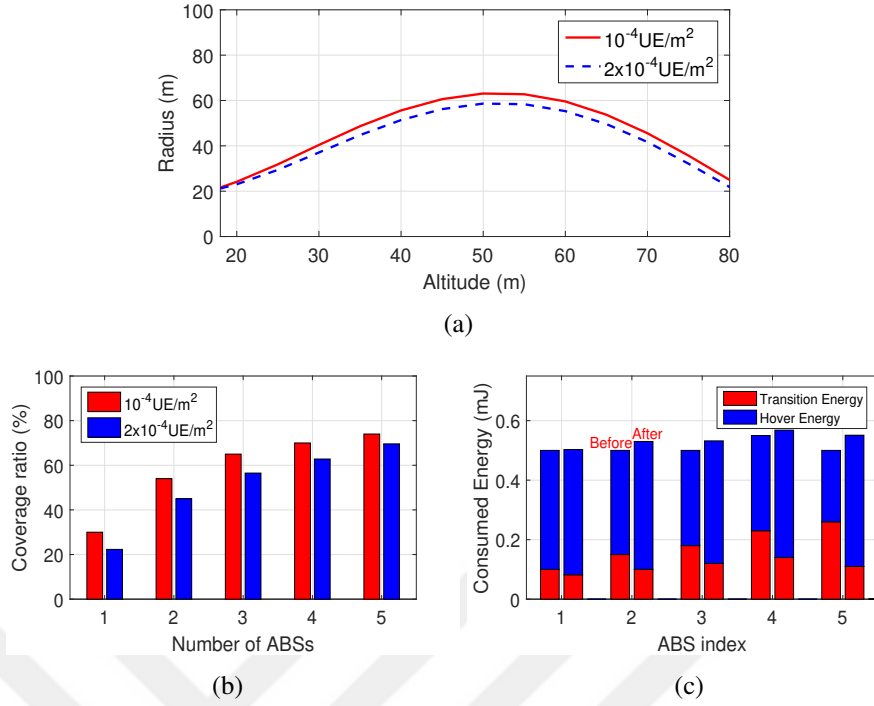


Figure 4.6 : (a) The relationship between coverage radius, $R_{cluster}$ and altitude (b) Coverage ratio with increasing number of ABSs (c) Consumed transition and hover energy before the first ABS deployment and after the update of location of control station.

traffic demands to satisfy users' QoS. Here, we consider the well-known D'Hondt Algorithm [61]- [62] (seat allocation) to assign Resource Blocks (RB) to the UEs and determine 'fair' allocation.

To explain the algorithmic method, we provide an example and show the implemented steps in Table 4.1. Assume that there are 9 unassigned RBs and 3 UEs with 10, 6 and 2 demands as seen in the 1st row. In this case, the existing RBs will not supply all traffic demands. All demands are listed for determining a fair allocation. There is also a divisor parameter, which initially is set to 1 for each UE. The 1st RB is allocated to UE_1 because of the highest demand. Then, the divisor is first incremented for UE_1 and then, the average demand is calculated as $\frac{demand}{divisor}$ as seen in the 2nd row. The divisor will not change for UE_2 and UE_3 . In the next step, the 2nd RB is allocated to UE_2 since UE_2 has now the highest average demand. Similarly, the divisor is first incremented for UE_2 and then, the average demand is calculated as $\frac{demand}{divisor}$ in the 3rd row. These processes continue until all resources are allocated, (i.e. $\lambda_i \leftarrow \lambda_i/2$, $\lambda_i \leftarrow \lambda_i/3$, and so on). In the end, UE_1 , UE_2 , and UE_3 allocate 5, 3, 1 RBs, respectively, as seen in the

Total row in the table. As a result, each division produces an average, and the ‘highest average demand’ is awarded to the available RB, until all RBs have been allocated.

Table 4.1 : Simulation for the allocation 9 RBs with 3 UEs.

Order of RB Allocation	Divisor (UE_1)	Average (UE_1)	Divisor (UE_2)	Average (UE_2)	Divisor (UE_3)	Average (UE_3)
1st	1	10	1	6	1	2
2nd	2	5	1	6	1	2
3rd	2	5	2	3	1	2
4th	3	3.33	2	3	1	2
5th	4	2.5	2	3	1	2
6th	4	2.5	3	2	1	2
7-9th	5	2	3	2	1	2
-	6	1.667	4	1.5	2	1
Total		5		3		1

4.3 Endurance Framework

Energy consumption of ABSs is of paramount importance for aerial networks since it directly affects the endurance and limits the network lifetime. In general, the consumed energy of an ABS is based on (i) transition power, P_{trans} , from initial location to designated location, (ii) hover power, P_{hov} , to serve UEs and (iii) communication power, P_{com} , with the control station. Minimizing each of them can help to extend ABSs’ lifetime.

With this purpose, each ABS independently maximizes the endurance (Υ). It is defined as the flight duration in the hovering state so that a higher hover energy leads to a higher endurance. The problem is considered as follows:

$$\Upsilon = \frac{E_{total} - [E_{trans(t_1-t_0)} + E_{trans(t_3-t_2)}]}{P_{hov}} \quad (4.7)$$

Accordingly, the optimization problem is to maximize the endurance as given in equation 4.8.

$$\max_{h_{min} \leq h^* \leq h_{max}, R_{cluster}} \Upsilon_j \quad \forall j \in M \quad (4.8)$$

subject to

$$C_1 : E_{res,ty} \geq \int_{t_2}^{t_3} P_{trans} dt \quad (4.9)$$

$$C_2 : \theta_j \in [\theta_{min} - \theta_{max}] \quad (4.10)$$

$$C_3 : a_{ij,ty} \in \{0, 1\} \quad (1 \leq i \leq U), (1 \leq j \leq M), (t_2 \leq t_y \leq t_3) \quad (4.11)$$

$$C_4 : \sum_{i=1}^U a_{ij,t} \leq 1 \quad (4.12)$$

where C_1 is the residual energy constraint, which will be detailed below. C_2 limits the relation between the altitude and coverage radius, where θ is the angle formed by the center of one of the circles and the points of intersection of the circles. C_3 states that if ABS serves the UE in the designated time slot t_y , $a_{ij,t_y} = 1$, otherwise $a_{ij,t_y} = 0$. Additionally, C_4 states that a UE cannot get service from more than one ABS in the designated time slot.

Total energy capacity of an ABS is given in equation 4.13:

$$E_{total} = \int_{t_0}^{t_1} P_{trans} dt + \int_{t_1}^{t_2} [P_{hov} + P_{com}] dt + \int_{t_2}^{t_3} P_{trans} dt \quad (4.13)$$

Accordingly, the hover power is given in equation 4.14:

$$P_{hov} = \frac{F^{3/2}}{\sqrt{2\rho A'}} \quad (4.14)$$

where $F = m_d g$, m_d is the ABS weight (kg), g is the earth gravity (m/s^2), and $A' = \pi r^2 m$, r is the radius of ABS's propellers and m is the number of drone's propellers. ρ is the air density (kg/m^3).

$$P_{hov} = \frac{(m_d g)^{3/2}}{\sqrt{2\pi r^2 m \rho}} \quad (4.15)$$

and

$$E_{hov} = \int_{t_1}^{t_2} \frac{(m_d g)^{3/2}}{\sqrt{2\pi r^2 m \rho}} dt \quad (4.16)$$

Transition energy is given in equation 4.3. However, the power consumption for the communication (P_{com}) is neglected to reduce the computation complexity.

E_{res,t_y} is the residual energy level of the ABS at time t_y and E_{con,t_y} is the consumed energy at time t_y where $t_1 < t_y < t_2$.

$$E_{res,t_y} = E_{max} - E_{con,t_y} \quad (4.17)$$

and

$$E_{con,t_y} = \int_{t_0}^{t_1} P_{trans} dt + \int_{t_1}^{t_y} P_{hov} dt \quad (4.18)$$

$$E_{res,t_y} \geq \int_{t_2}^{t_3} P_{trans} dt \quad (4.19)$$

In order to manage ABSs, we introduce Algorithm 3. The principle is to track the residual energy of ABSs in each time slot and give a decision for recharging. After

decision to recharge, we calculate the consumed energy as given in equation 4.18, thereby, the lower the consumed energy, the quicker the charging time. Then, each ABS is either assigned to one of the replenishment stations or programmed to the sleeping state. Each ABS needs to execute Lines 2-3 of the Algorithm 3 per discrete time slot and this takes $O(1)$ operations. Similarly, Lines 4-7 are $O(1)$. Thus, total complexity is $O(n)$ operations per discrete time.

Algorithm 3: Maximizing Endurance

```

1 for  $j \leftarrow 1$  to  $M$  do
2    $E_{res,t_{y+1}} \leftarrow \text{compute } \forall j \in M$ 
3    $E_{threshold} \leftarrow \int_{t_2}^{t_3} P_{trans}(t)$  //Please note that the location of control station is updated
    in Algorithm 2
4   if  $E_{res,t_{y+1}} < E_{threshold}$  then
5     Schedule for charging
6      $w_j \leftarrow E_{con,t_y}$ 
7   end
8 end
9 Sort ABS according to  $w_j$  in ascending order
10 Select the ABSs in order for recharging

```

4.4 Path Planning

Path planning of ABSs is of paramount importance to manage the operations of ABSs and reduce energy consumption in the topology. In this section, we focus on a path planning strategy to minimize the consumed energy when an ABS's battery needs to be recharged.

The problem definition is illustrated in Figure 4.7. As seen in the Figure 4.7(a), after ABS deployment, a weighted graph is constructed, where $G = (V, E, w_{ij})$, V and E represent the ABSs and the connections among ABSs with positive weights, respectively. For a given κ , the weight of each edge is at most κ . Weights are the distance between ABSs and if $w_{ij} \leq \kappa$, then ABS_i and ABS_j are neighbor nodes.

In Figure 4.7(b), we show the scenario to explain the path planning strategy. Assume ABS_1 needs to recharge its battery and it will be directed to the ground control station for the replenishment. Before the transition, the controller computes the consumed transition energy from ABS_1 's location to the ground control station. We refer to it as E_1 . Then, the controller calculates the possible consumed energies when the ABSs' locations are updated as showed in the Figure 4.7(b). Instead of directing a new

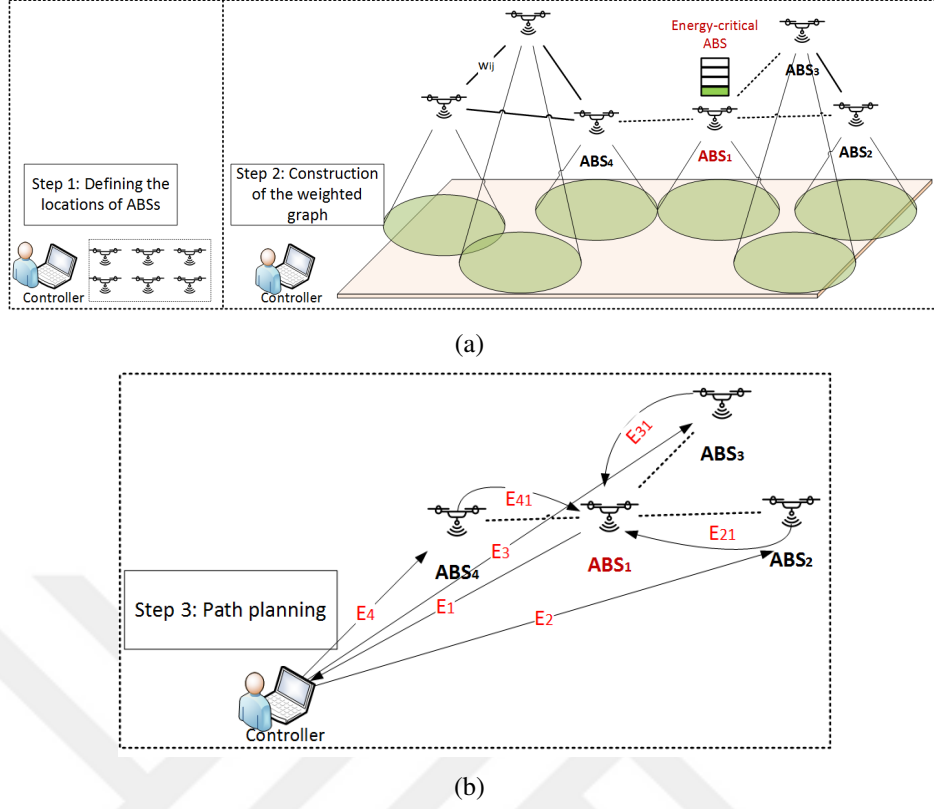


Figure 4.7 : Illustration of path planning (a) ABS deployment and construction of the weighted graph (b) Possible path planning processes.

ABS to the ABS_1 's location, we explore feasible solutions to minimize the consumed energy over the existing network topology. For instance, one of the possible approach is that we show the consumed energy when ABS_2 moves to the location of ABS_1 , (E_{21}) and when the new deployed ABS is directed to the existing location of ABS_2 , (E_2). The planning process reacts to the changes in not only energy-critical ABS but also neighbor ABSs. The controller makes all calculations and updates the ABSs' locations. Another possible approach can be between ABS_3 and ABS_1 , and ABS_4 and ABS_1 . More specifically, the controller calculates $\min\{E_1, \min\{E_2 + E_{21}, E_3 + E_{31}, E_4 + E_{41}\}\}$. The basic problem is to find a feasible path by minimizing total consumed energy in the network so there is need to identify the locations of ABSs dynamically.

Thus, the optimization problem aims to minimize the consumed energy for all ABSs as given in equation 4.20 and Algorithm 4 gives the steps to implement this solution.

$$\min \sum_{i=1}^N E_{con} x_i \quad (4.20)$$

subject to the following constraints:

$$E_{res,tx} \geq E_{con} \quad (4.21)$$

$$x_i \in \{0, 1\} \quad (4.22)$$

where equation 4.21 states that residual energy of the ABS should be higher than the transition energy that will be consumed for transfer where $E_{res,t_x} = E_{max} - E_{con,t_x}$. Equation 4.22 states that $x_i = 1$ if ABS is scheduled for the replenishment at t_{x+} , otherwise $x_i = 0$. In order to find the consumed transition energy from the initial location to the designated location and vice versa, we use equation 4.18.

Algorithm 4: Path Planning

```

1 ABSDeployment()
2 Construct  $G = (V, E, w_{ij})$  such that  $w_{ij} \leq \lambda$ 
3 Controller triggers to  $ABS_i$  for battery recharging
4 for each neighbor  $ABS_j$  do
5   | Compute  $\min\{E_i, \min\{E_j + E_{ij}\}\}$ 
6 end
7 Select the combination of min. energy consumption
8 Update  $(x, y, z)$  locations for ABSDeployment()

```

4.5 Scheduling between ABSs and Replenishment Stations

In equation 4.19, the controller follows the residual energy after the ABS is at the hovering state and accordingly, gives a decision for recharging based on the threshold energy level. Please note that threshold energy level is different for each ABS and calculated in Algorithm 3. If the number of ABSs that needs to be recharged is more than the number of available replenishment stations, there should be a scheduling mechanism. In this case, these ABSs wait in the sleeping state to be recharged as illustrated in Fig. 4.8. Thus, in the proposed model, the controller presents a strategy to schedule the ABSs' operations.

With the proposed approach, the control station starts scheduling with the first arrival of ABS to the replenishment stations and, then updates the system when a new arrival or departure occurs with equations 4.23-4.24.

$$L = \sum_{n=1}^T \tau(t_n - t_{n-1}) / T \quad (4.23)$$

and

$$W = \sum_{t_a, t_d \in T} [t_d - t_a] / M' \quad (4.24)$$

where L and W are the mean number of the ABSs and mean charging time (*min*) in the replenishment station. τ and M' represent the number of ABSs at time t and the

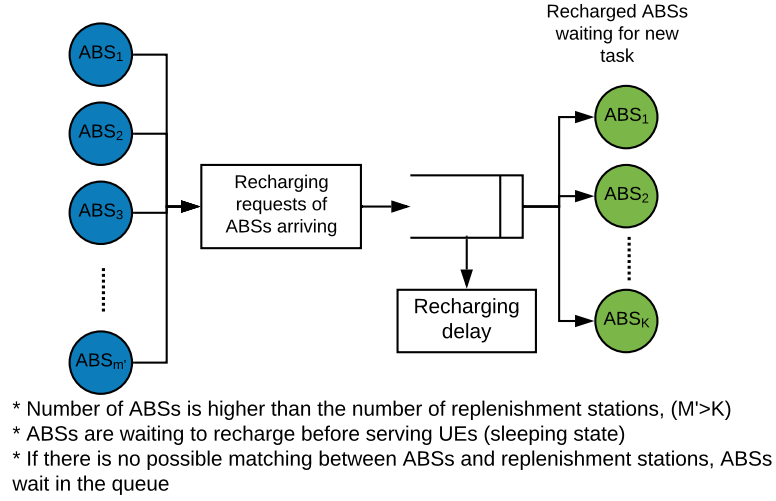


Figure 4.8 : Recharging requests of ABSs.

total number of arrival over the time period $[0, T]$. t_a and t_d are arrival and departure times of the ABSs in the system. This also shows the charging time of an ABS, where $[t_d - t_a](min) = CE_{con}/I_c E_{max}$, C (in mAh) is the capacity of the battery and I_c (in Ampere) is the current of the charge.

For example, let us consider the illustration in Figure 4.9(a). The number of the ABSs that arrives to the station for recharging over the time period $[0, T]$ is $M' = 4$. Black circles show the arrivals and red circles show the departures. L and W parameters are given in Equations 4.25-4.26 [63].

$$\begin{aligned}
 L &= [1(t_2 - t_1) + 2(t_3 - t_2) + 1(t_4 - t_3) + 2(t_5 - t_4) + 3(t_6 - t_5) + 1(T - t_6)]/T \\
 &= [T + 2t_6 - t_5 - t_4 + t_3 - t_2 - t_1]/T
 \end{aligned} \tag{4.25}$$

$$\begin{aligned}
 W &= [(t_3 - t_1) + (t_6 - t_2) + (t_6 - t_4) + (T - t_5)]/K \\
 &= [T + 2t_6 - t_5 - t_4 + t_3 - t_2 - t_1]/4
 \end{aligned} \tag{4.26}$$

However, if we assume that the number of replenishment stations is equal to $R = 2$, as seen in Figure 4.9(b), it cannot be possible to recharge ABS_4 at time t_5 so that ABS_4 waits in the sleeping state until t_6 . Thus, we propose a scheduling mechanism to minimize the waiting times of ABSs for recharging under the assumption of the limited number of replenishment stations as given in Algorithm 5. Algorithm 5 runs with the first arrival and tracks the busy periods of the replenishment stations ($[t_a, t_d]$) over the time period $[0, T]$. If there is no available station, then busy periods are computed in

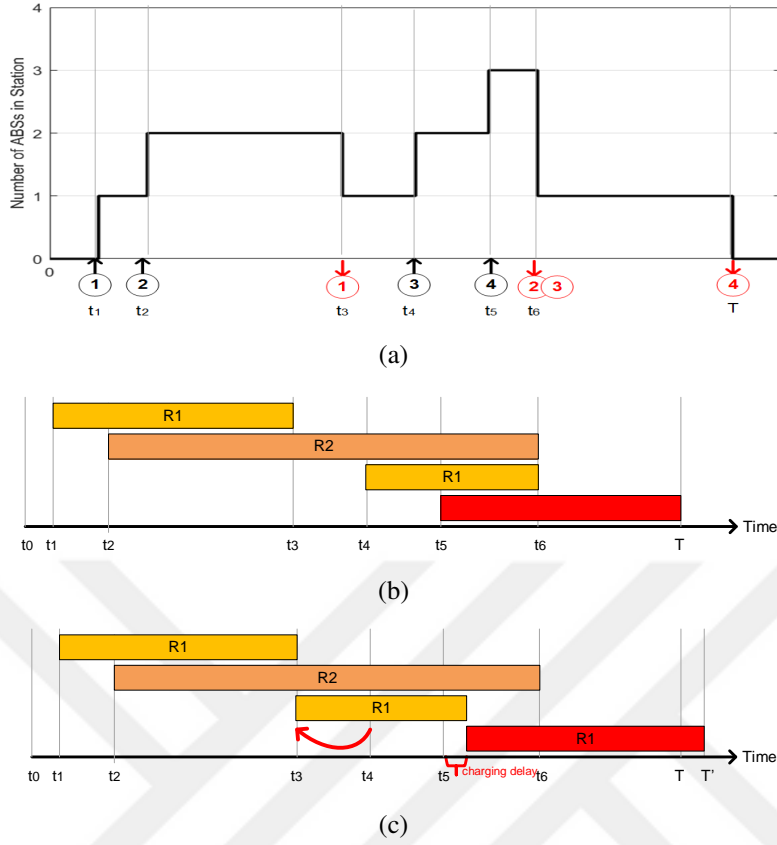


Figure 4.9 : (a) Illustration of busy period of replenishment station (b) Before scheduling (c) After scheduling.

the case of early arrival (Lines 7-13) and accordingly, the task is updated by the control station.

As seen in Figure 4.9(c), the task of ABS_3 is updated and then ABS_3 is ready for recharging at time t_3 so that ABS_4 is now scheduled after the departure of ABS_3 . Another approach could be to update the task of ABS_2 . However, in this case, we assume that $t_6 - t_4 + t_3 < t_6 - t_2 + t_1$. This is controlled in Algorithm 5. Let us now discuss the computational complexity of implementing Algorithm 5. Each ABS that arrives to the station for recharging executes this procedure with $O(n)$ operations. Each line between 3 to 7 is accomplished with $O(1)$ operations per discrete time step. For the worst case scenario, all ABSs wait for recharging and replenishment stations are busy. The total complexity is $O(n)$ operations between lines 8-10. Similarly, each line between 11 to 13 is accomplished with $O(1)$ operation per discrete time step. Thus, the total complexity is $O(n^2)$ operations.

Algorithm 5: Scheduling for Recharging

```
1 Sort ABSs by arrival time over the time period [0,T] so that  $t_{a1} \leq t_{a2} \leq \dots \leq t_{aK}$ 
2 for  $j \leftarrow 1$  to  $M'$  do
3   if  $ABS_j$  is compatible with a station  $r$  then
4     Schedule  $ABS_j$  to the station  $r$ 
5      $[t_{aj}, t_{dj}] \leftarrow$  compute busy periods for  $r \in R$ 
6      $t(r) \leftarrow t_{dj}$  // station  $r$  is busy until  $t_{dj}$ 
7   else
8     for  $r \leftarrow 1$  to  $R$  do
9       new  $(t(r)_{dj}^*) = t(r)_{dj} + t(r)_{aj-1} - t(r)_{aj}$ 
10    end
11    Select min(updated  $(t(r)_{dj}^*)$ )
12    Update the task of  $ABS_j$ 
13    Allocate station  $r$  at first available  $(t(r)_{dj}^*)$  and schedule  $ABS_j$  to the
      defined station
14  end
15 end
16 end
```

4.6 Handover Procedure

A handover procedure mainly involves handover preparation, handover decision, handover execution, and handover completion stages. All these stages come at a cost to aerial networks and complexity rapidly increases. Since handovers result in signaling overhead [50], the handover procedure is an important indicator to evaluate the aerial network performance [45]- [64]. Frequent handover decisions and execution consume more energy adding overhead to the ABSs that also affect flight endurance. Handover delay and packet loss during the handover process may cause serious degradation of system performance [64].

We implement an RL framework, where the controller learns how to manage ABSs and maximize the number of served UEs. As seen in Figure 4.10, the agent (controller) interacts with the environment and receives feedback so that it finds the optimal policy to deploy ABSs.

4.6.1 Markov decision process

Let $S = \{s_1, s_1, \dots, s_n\}$ denote the state space and $A = \{a_1, a_1, \dots, a_m\}$ denote the action set. Agent takes an action, a_t at time t according to current state, s_t , then, the system

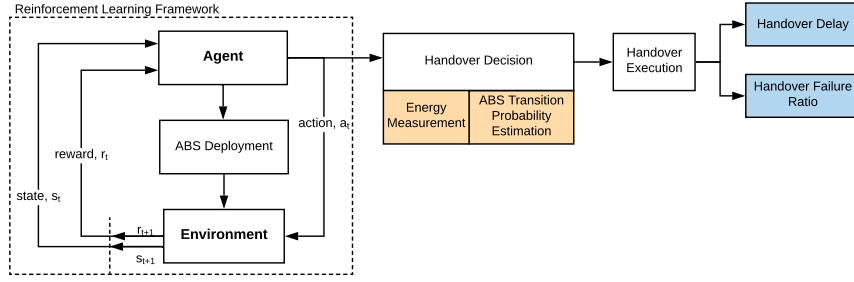


Figure 4.10 : Energy-aware handover mechanism.

obtains a new state for the time $t + 1$ with the transition probability P and obtains a reward, $r = \sum_{i=1}^M U_i$, where U_i is the number of served UEs by ABS_i . Agent obtains the measurement from the environment with the help of ABSs. ABS serves the UEs within the coverage area. The decisions about how to move ABSs in the target area are given by the controller based on the current energy level of the ABSs. The agent manages the ABSs whether the ABS should (1) change the position, (2) remain stationary and continue to serve the UEs in the same coverage area, or (3) transit to the ground to recharge its battery. Thus, we assume that ABSs have three actions and the states are determined by the state of the battery, *low*, and *high*.

Let us define the possible combinations, $A = \{change, wait, recharge\}$ and $S = \{low, high\}$. A period of changing position that begins with a *high* energy level leaves the energy level *high* with probability α and reduces it to *low* probability $1 - \alpha$. Similarly, a period of waiting at the position that begins with a *high* energy level leaves the energy level *high* with probability β and reduces it to *low* with probability $1 - \beta$. When the energy level is *low*, ABS should be directed to the ground for recharging. Accordingly, action sets are $A(high) = \{change, wait, recharge\}$ and $A(low) = \{recharge\}$. Reward is computed based on the number of served UEs in the coverage area. We summarize the transition probabilities in Table 4.2 and Figure 4.11 shows the transition graph.

Table 4.2 : Transition probabilities.

s	a	s'	$P(s' s,a)$	$R(s,a,s')$
high	change	high	α	r_{change}
high	change	low	$1 - \alpha$	r_{change}
high	wait	high	β	r_{wait}
high	wait	low	$1 - \beta$	r_{wait}
high	recharge	high	1	0
high	recharge	low	0	0
low	recharge	high	1	0
low	recharge	low	0	0

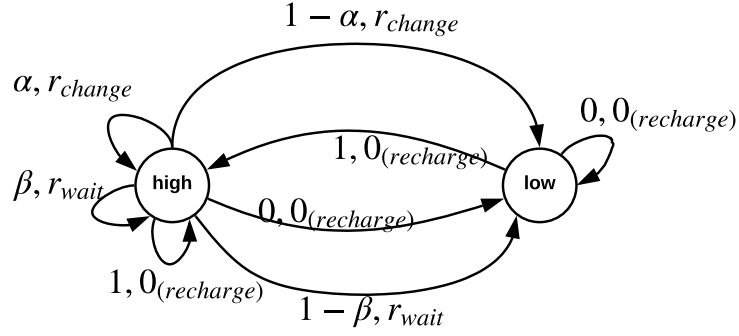


Figure 4.11 : Transition graph.

The goal of the agent is to maximize the total rewards under a policy π . The value of a state, s and the value of taking action a in this state are defined in Equations 4.27-4.28, respectively [65].

$$V_{\pi}(s) = \mathbb{E}_{\pi}(G_t | S_t = s) = \mathbb{E}_{\pi}\left(\sum_{k=0}^{\infty} \gamma^k R_{t+k+1} | S_t = s\right), \forall s \in S \quad (4.27)$$

and

$$Q_{\pi}(s, a) = \mathbb{E}_{\pi}(G_t | S_t = s, A_t = a) = \mathbb{E}_{\pi}\left(\sum_{k=0}^{\infty} \gamma^k R_{t+k+1} | S_t = s, A_t = a\right) \quad (4.28)$$

where $\mathbb{E}_{\pi}[\cdot]$ is the expected value of a random variable.

The problem is to find a control policy that specifies how each ABS serves the maximum number of UEs and this is achieved with an optimal policy, π^* . Thus, the optimal state value function is denoted V^* and is as follows.

$$V^*(s) = \max_{\pi} V_{\pi}(s), \quad \forall s \in S \quad (4.29)$$

Similarly, optimal action value function is defined as follows.

$$Q^*(s, a) = \max_{\pi} Q_{\pi}(s, a), \quad \forall (s \in S \ \& \ a \in A(s)) \quad (4.30)$$

To learn the optimal action value, we define the function as a Bellman equation that gives the value of a state under an optimal policy, π^* must be equal to the expected return for the best action from that state [65]. Bellman equations are given for V^* and

Q^* in Equations 4.31-4.32, respectively.

$$\begin{aligned}
V^* &= \max_{a \in A(s)} Q_{\pi^*}(s, a) \\
&= \max_a \mathbb{E}_{\pi^*}[G_t | S_t = s, A_t = a] \\
&= \max_a \mathbb{E}_{\pi^*}[R_{t+1} + \gamma V^*(S_{t+1} | S_t = s, A_t = a)] \\
&= \max_a \mathbb{E}_{\pi^*}[R_{t+1} + \gamma V^*(S_{t+1} | S_t = s, A_t = a)] \\
&= \max_a \sum_{s', r} p(s', r | s, a) [r + \gamma V^*(s')] \tag{4.31}
\end{aligned}$$

and

$$\begin{aligned}
Q^*(s, a) &= \mathbb{E}[R_{t+1} + \gamma \max_{a'} Q^*(S_{t+1}, a') | S_t = s, A_t = a] \\
&= \sum_{s', r} p(s', r | s, a) [r + \gamma \max_{a'} Q^*(s', a')] \tag{4.32}
\end{aligned}$$

4.6.2 TD learning prediction: Q-learning

The proposed model is based on TD learning prediction: Q-learning algorithm. This method is executed according to an update procedure. The algorithm calculates an update reward at each time for each state, s_t and action, a_t as follows [66]:

$$Q(s_t, a_t) \leftarrow Q(s_t, a_t) + \phi [r_{t+1} + \gamma \max_a Q(s_{t+1}, a) - Q(s_t, a_t)] \tag{4.33}$$

where $0 < \phi < 1$ is the learning rate, $0 < \gamma < 1$ is the discount rate. This update is done after every transition and follows the rule as given in equation 4.33. Q-learning includes an agent with a set of states and a set of actions per state. Here, the actions are defined according to Q value for each state-action pair. Q function calculates a reward value at each episode for state, s_t and action, a_t pair to find best control policy as given in Algorithm 6.

Algorithm 6: Q-learning Algorithm

```

1 Initialize  $Q(s, a) \forall s \in S, a \in A(s)$  and  $Q(s, a) = 0$ 
2 while until terminated do
3   Initialize S
4   while until terminated do
5     Choose A from S using greedy policy
6     Take action A and observe r and next state  $s'$ 
7      $Q(s, a) \leftarrow Q(s, a) + \phi [r + \gamma \max_a Q(s', a) - Q(s, a)]$ 
8      $s \leftarrow s'$ 
9   end
10 end

```

4.6.3 Handover decision

In the considered scenario, after ABS deployment, the control station monitors the energy level of ABSs and defines the battery recharging time. Whenever an ABS needs to be changed, the control station sends a new ABS to the designated position/ updates the positions. The new ABS is then configured to take over the wireless service using X2 interface. The UE contexts are transmitted from serving ABS to the target ABS. Similarly, a mobile UE can move out of the coverage area and it can be assigned to a new ABS. In this case, accurate knowledge of the mobile UE's context is transferred to the target ABS. If the connection is established with the new ABS before breaking the connection from the old ABS, it is also referred as seamless handover [64]. In this section, we present the handover procedure in terms of the handover decision and handover execution.

Controller decides whether to switch the user to the target ABS based on the Time-to-Trigger (TTT) parameter. Accordingly, handover procedure is triggered when the following condition is satisfied for more than TTT seconds [67].

$$RSRP_{serving} - RSRP_{target} > HYS \quad (4.34)$$

where RSRP is the Reference Signal Receive Power and HYS is the Handover Hysteresis Margin.

Because of the limited battery capacity, battery recharging is inevitable in aerial networks to serve UEs continuously. This results in frequent handover with additional problems related to increased delay and failure. The consumed energy of ABSs is followed to decide the time for exchange. The energy calculations cause additional overhead to the ABSs and result in more energy consumption. Thus, it is important to manage ABSs intelligently from a control station perspective. With this idea, one of the main tasks of the control station is to follow the consumed energy of the ABSs and decide the exchange periods. In the case of ABS battery depletion, we show the procedure in Figure 4.12.

Handover decision is given by the control station based on the measurement reports of the ABSs and the decision process is given in Algorithm 7 by following the residual energy of ABSs, E_{res} . Accordingly, the consumed transition energy, E_{trans} , as given in Equation 4.3, from designated location to the control station for recharging is

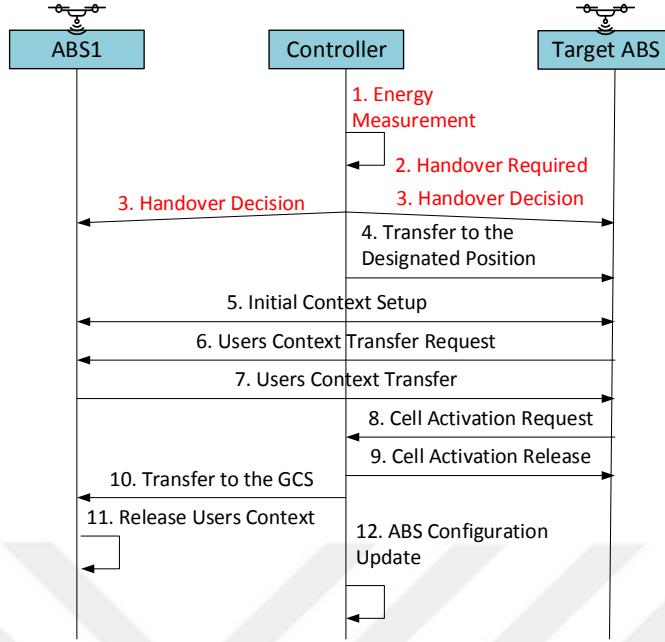


Figure 4.12 : In the case of ABS battery depletion.

calculated. Please note that ABSs are directed to the control station along a flight path by minimizing the travel length.

Algorithm 7: ABS Handover Decision

```

1 for  $i \leftarrow 1$  to  $M$  do
2    $E_{res,(t+1)} \leftarrow \text{compute } \forall i \in M$ 
3    $E_{threshold} \leftarrow \left( \frac{P_{full} - P_s}{v_{max}} v_d + P_s \right) t$ 
4   if  $E_{res,(t+1)} < E_{threshold}$  then
5      $\text{HandoverDecision}()$  //Switch the ABS with a new ABS
6      $\text{HandoverExecution}()$ 
7   end
8 end

```

4.6.3.1 ABS transition probability estimation

In the case that a UE moves out from the range of current ABS, we show the handover procedure in Figure 4.13. In general, if we assume that a UE is currently in the ABS_i , the process starts with state s_i and moves from this state to the candidate states, s_j or stay in the same state with the transition probability, P_{ij} . Accordingly, mobile UEs on each cell will have transition probabilities with the ABS deployment. Cell transitions are modeled with Markov chain [68] as shown in Figure 4.14.

Transition probability matrix, \mathbb{P} consists of elements P_{ij} , that is: $\mathbb{P} = [P_{ij}]$. The state space is the set of the squares of the ABSs. Since UEs can move to neighbor ABSs in

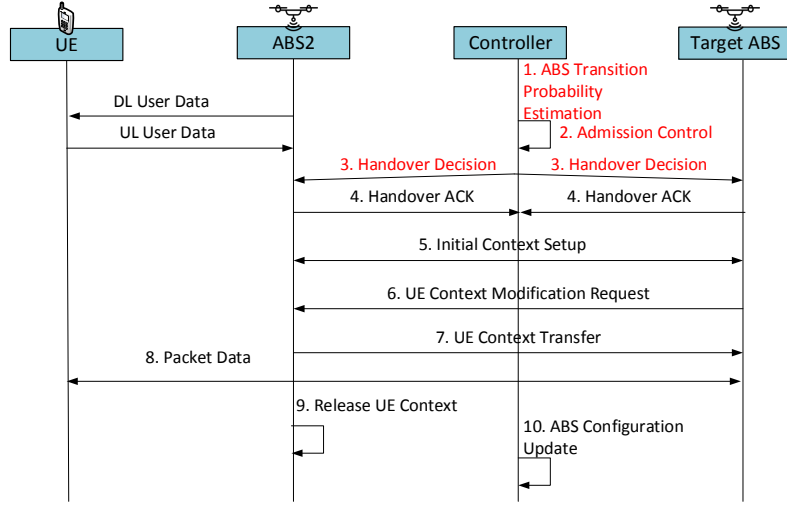


Figure 4.13 : Handover procedure with ABS transition probability estimation.

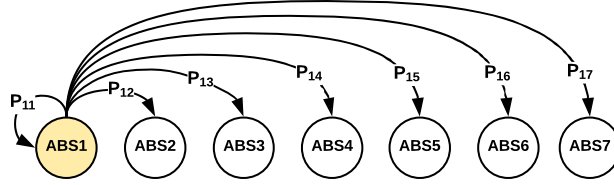


Figure 4.14 : Markov chain for the transition probabilities.

some unpredictable fashion, the position of a UE at some time in the future is a random variable [69]. When $X_t = j$ (it means that the UE is in the ABS_j at time t), then the system is said to be in state s_j at time t . To start the procedure, we assume that the UE started at $t = 0$ with some initial probability distribution, $\mathbb{P}[X_0 = j]$ as follows.

$$P_{ij} \triangleq \mathbb{P}[X_t = j | X_{t-1} = i] \quad (4.35)$$

Equation 4.35 gives the probability of being in state s_j on the next movement, given that the UE is currently at state i . Thus, the current state depends only upon the state, not upon the current time. The n-step transition probability is defined as follows:

$$P_{ij}^{(n)} \triangleq \mathbb{P}[X_{t+n} = j | X_t = i] \quad (4.36)$$

From the Markov property, to calculate $P_{ij}^{(n)}$, equation 4.37 can be established.

$$P_{ij}^{(n)} = \sum_k P_{ik}^{(n-1)} P_{kj} \quad n = 2, 3, \dots \quad (4.37)$$

Then, we define the probability vector as follows:

$$\pi_j = \sum_{i \in S} \pi_i P_{ij} \quad (4.38)$$

where $\sum_i \pi_i = 1$ and P_{ij} is as follows:

$$P_{ij} = \begin{cases} \frac{1}{N(i)}, & \text{if cell } j \text{ is a neighbor of cell } i \\ 0, & \text{otherwise} \end{cases} \quad (4.39)$$

where $N(i)$ is the number of possible next states in i^{th} cell. We demonstrate the relationship among ABSs with an adjacency matrix, $D = \{d_{ij}\}$, where d_{ij} is equal to 1 if ABS_i and ABS_j are neighbor. Otherwise, $d_{ij} = 0$.

4.6.4 Handover execution

When a mobile UE moves out of the range of current *ABS*, target *ABS* allocates the resource for the specific UE as shown in Figure 4.13. After the handover decision is given by the control station, the procedure involves the connection between *ABS*s, transfer of UE context over X2 backhaul interface, and updating S1 Application Protocol (S1AP) path routing [70]. Serving *ABS* initiates the procedure. Then, target *ABS* initiates the UE context transfer request sending *USER CONTEXT RELEASE* message and triggers the release of resources [71]. When serving *ABS* receives the message, it transfers the users' context. Once the handover is completed, serving *ABS* releases the wireless service associated to the UE. At that time, both serving *ABS* and target *ABS* receives uplink user data. After it is confirmed, serving *ABS*₁ now stops uplink reception and releases related resources.

5. EVALUATION OF THE STUDY

In this chapter, we extensively evaluate the effectiveness of *AirNet*. To analyze this, we first consider four different schemes to deploy ABSs under the constraint of limited number of ABSs: (i) Random ABS deployment (ii) ABS deployment to the locations of damaged BS (iii) Set cover approach (iv) Energy-aware ABS deployment. Then, we verify the benefits of an optimized scheduling of the ABSs' visits to the replenishment stations.

5.1 Simulation Setup

The performance is evaluated by the simulation environment as seen in Figure 5.1. Windows 10 operating system is chosen with Cygwin software for the ABS control using STIL ArduPilot simulator [60] and MAVProxy 1.5.0. STIL allows to create and test drones without a real vehicle using C++ compiler. We also use MATLAB & Simulink for the proposed model in the controller.

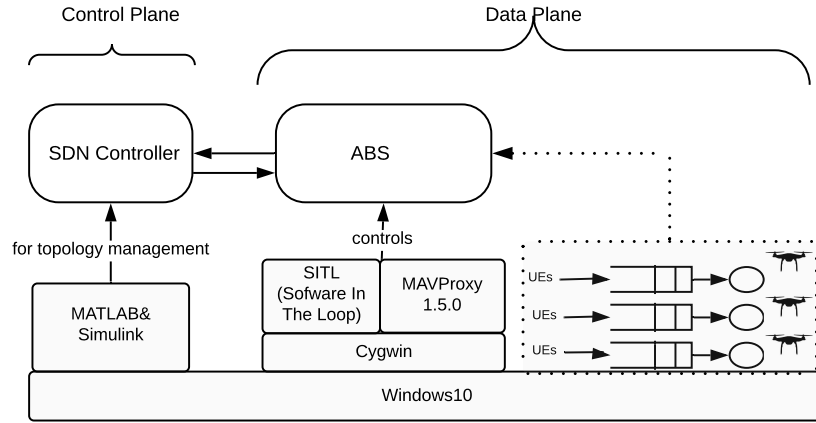


Figure 5.1 : Simulation environment.

In our simulation, we consider ABS-based communication for urban environment over $2GHz$ carrier frequency with $a = 4.2$, $b = 8$, $k_1 = 10.39$, $k_2 = 0.05$, and $g_1 = 29.06$, $g_2 = 0.03$ [52], [55]. UEs are uniformly distributed with $\lambda_u = 4 \times 10^{-2} UEs/m^2$ in 50×50 cells, where the length of each cell is $20m$. UEs are moving with the speed $3km/h - 10km/h$ according to Random Waypoint (RWP) mobility model. We assume

that ABS transmission power is $P_t = 24dBm$, battery capacity is $2 \times 10^4 mAh$, average (v_d) and maximum speed (v_{max}) are $10m/s$ and $20m/s$, respectively. An ABS transmits at power level with full speed $P_{full} = 5W$ and when $v_d = 0$, $P_s = 0$. It is assumed that ABS weight is $m_d = 650g$ with $m = 4$ propellers, air density is $\rho = 1.125kg/m^3$ and charge rate current is $2.4A$.

5.2 Benefits of Energy-Efficient Deployment

As the baseline ABS deployment comparison, we analyze 4 different approaches with 10 ABSs as follows.

- *Random ABS deployment:* We randomly deploy the ABSs to the target area with the same coverage radius ($R_{cluster} = 50m$).
- *ABS deployment to the locations of damaged BS:* We deploy the ABSs to the locations of damaged BS at fixed height ($h = 60m$).
- *Set cover approach:* As a baseline comparison, we analyze the study in [52]. In this scheme [52], the circle packing approach is considered to cover a target area and then the authors compute the coverage utility and coverage radius. We made some changes in this study to apply our scenario. First, we consider the target region as a square area instead of a circular area. Then, we focus on covering the entire target area. To exemplify this, Figure 5.2 is given with 10 and 15 ABSs. As seen in the figure, when the required number of ABSs changes, the coverage radius shows a difference. By considering this approach, we create the circles to cover all target area with the same radius ($R_{cluster} = 50m$) since [52] considers the fixed circles. Then, we consider the set cover problem that selects the set with maximum number of UEs under the constraint of limited number of the ABSs.
- *Energy-aware ABS deployment:* *AirNet*, which was presented in the Chapter 4.

In Figure 5.3, we set the number of ABSs as 10 and show the coverage areas for 4 different approaches, respectively. First, we randomly deploy the ABSs in Figure 5.3(a) and analyze coverage utility for the target area. Then, in Figure 5.3(b), it is assumed that terrestrial BSs are located with the distance of $200m$ in the target area and we deploy ABSs to these locations at the fixed height, $h = 60m$. Since

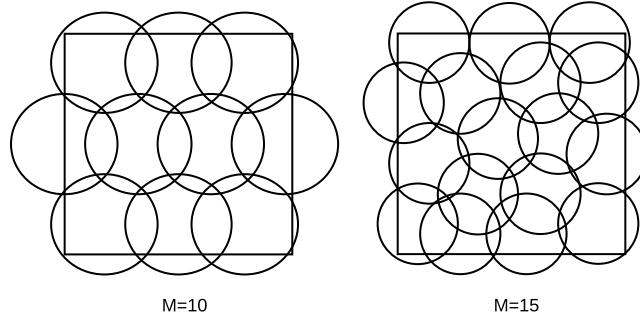


Figure 5.2 : Covering a given target area with $M=10$ ($R_{cluster} = 0.2182a(m)$) and $M=15$ ($R_{cluster} = 0.1796a(m)$).

it is not possible to cover all UEs within the coverage area of a terrestrial BS, we deploy the ABSs to maximize the number of covered UEs. At each step, we select the sets which have maximum number of UEs. In Figure 5.3(c), we mainly focus on the prior work [52] as a baseline that uses ABSs to provide wireless coverage in a given geographical area. We initially consider coverage problem with circles, $R_{cluster} = 50m$ and we define the required number of circles to cover target area as explained in [72]. Then, we focus on the set cover problem since we assume that the number of ABSs is limited and we select the circles that maximize the number of covered UEs. Finally, in Figure 5.3(d), we show the proposed energy-aware ABS deployment and evaluate the results. Please note that after ABS deployment, the comparisons will show how the algorithms reflect the performance evaluation in terms of the coverage utility, consumed transition energy, throughput, and recharging delay.

Figure 5.4 shows the coverage utility with the deployment of 10, 15, 20, and 25 ABSs. Coverage utility is the ratio of covered UEs to the all UEs. We see that when the number of ABSs increases, *AirNet* provides the best results, it also outperforms the set cover approach. Energy-aware deployment adjusts maximum coverage area with the minimum required transmission power in Algorithm 1 and enables average 24% and 3.72% increase in the coverage utility when compared to the random and set cover approach [52], respectively. As seen in the figure, random and deployment to the locations of damaged BS are not directly applicable for a potential solution in the mission critical environments.

After energy-aware ABS deployment, we next investigate the consumed transition energy for 10 ABSs in Figure 5.5. The transition energy from the control station to the designated location ($E_{trans} = \int_{t_0}^{t_1} P_{trans} dt$) and from the designated location to the

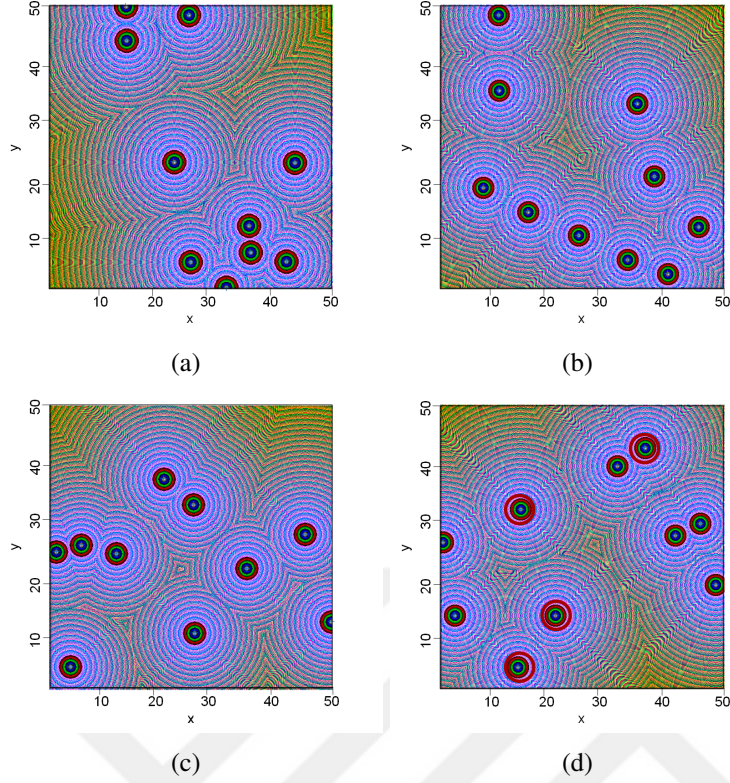


Figure 5.3 : ABS deployment for different schemes with 10 ABSs (a) Random ABS deployment (b) ABS deployment to the locations of damaged BS (c) Set cover approach (d) Energy-aware ABS deployment.

control station for recharging ($E_{trans} = \int_{t_2}^{t_3} P_{trans} dt$) are analyzed, where equation 4.3 gives the details. Initially, the control station was located at $(0,0,0)$ in the axes and ABSs are directed to the designated locations (x_j, y_j, h_j) . Then, the position of the control station is adaptively updated with Algorithm 2 and we compute the consumed transition energy for individual ABSs so that the hover time is increased 8% in the aerial networks.

5.3 Demand-Aware Reconfiguration

Since user demand can vary over time in an unpredictable way, this motivates us to analyze the demands as variable and also not known. Therefore, we assume that the packet arrival rate is $\lambda_i = 60 \text{ packets/sec}$ with Poisson distribution and the packet size distribution has a power law behavior with mean 1100 bytes to design an efficient traffic model. Power-law distribution is used to characterize the equilibrium of the users' demands. Under the packet size distribution and availability of the existing resources, demand-aware reconfiguration enables a fair resource allocation. In this respect, in Figure 5.6, we show the total throughput with respect to average hover

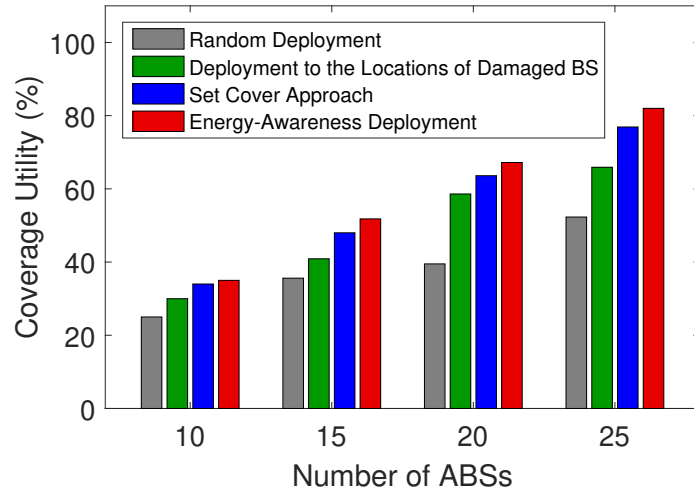


Figure 5.4 : Coverage utility for 4 different schemes.

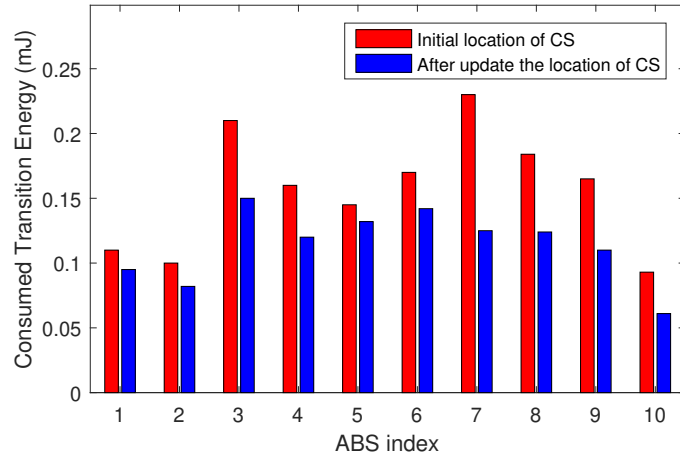


Figure 5.5 : Consumed transition energy of individual ABSs.

time with 10 and 15 ABSs. More importantly, it is shown that when the number of ABSs is increased, the proposed model enables significant improvement thanks to demand-aware reconfiguration and the rate does not increase the same rate for different schemes.

5.4 Benefits of Scheduling

Under the assumption of the limited number of replenishment stations, in order to observe the benefits of the scheduling mechanism, Figure 5.7 shows the normalized recharging delay before and after scheduling approaches according to different number of replenishment stations. Recharging delay is defined as the waiting time before recharging. In order to provide a clearer illustration, recharging delay is independently

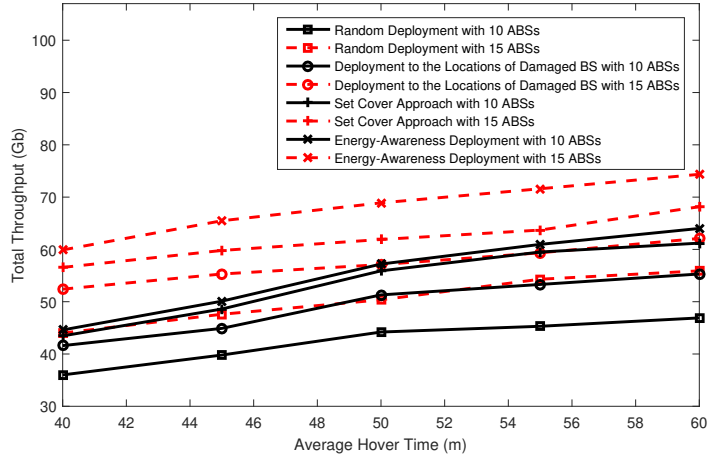


Figure 5.6 : Average hover time w.r.t. total throughput.

normalized for different number of stations. The results are obtained with respect to the increasing number of ABSs. Note that we only focus on ABSs that wait in recharging state. The benefit of providing a scheduling between the ABSs and stations is seen from the figure, when the number of stations increases, the results indeed outperform greatly. Thus, to obtain the results for the scheduling mechanism, we first compute the mean number of ABSs and mean charging time in the replenishment station over the simulation time as shown in Figures 5.8(a)-5.8(b) with equations 4.23-4.24, respectively so that we can evaluate the recharging delay. In Figure 5.8, we assume that there are 4 stations with respect to the changing number of ABSs. As expected, when the number of ABSs that needs to be recharged is higher than 4, the construction of the scheduling mechanism will be very useful to guarantee a better network management.

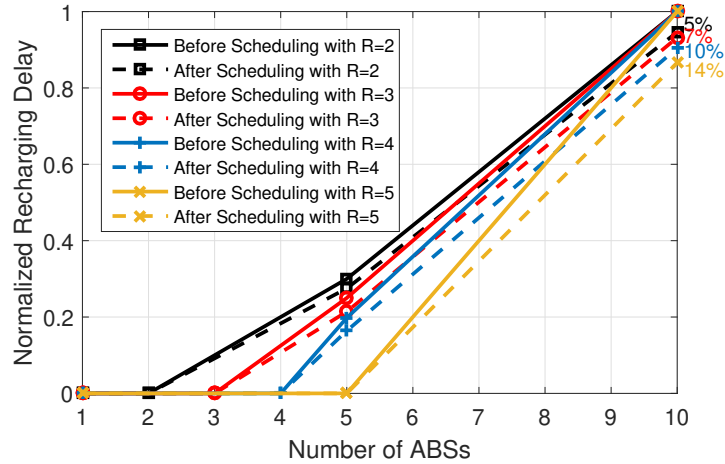
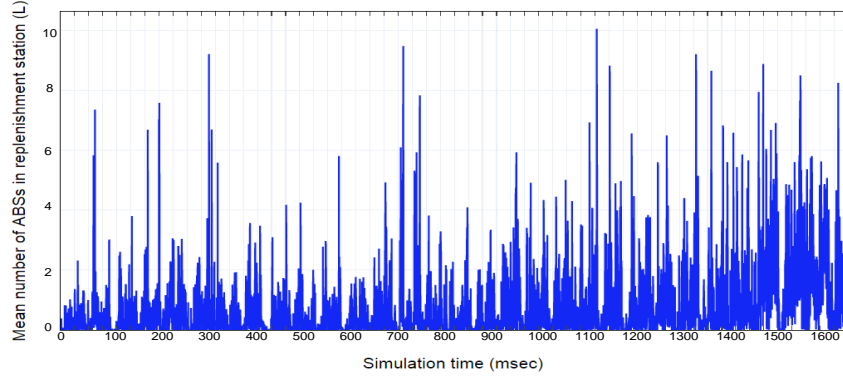
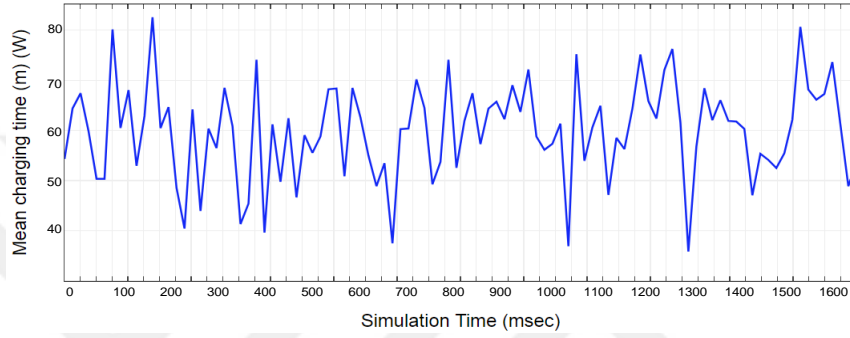


Figure 5.7 : Normalized recharging delay before scheduling and after scheduling with different number of replenishment station.



(a)



(b)

Figure 5.8 : (a) Mean number of ABSs and (b) Mean charging time in the replenishment station.

Next, we demonstrate the Probability Density Function (PDF) of recharging delay for 2, 3, 4 and 5 replenishment stations for one ABS in Figure 5.9. Note that, in order to obtain reliable simulation estimates, we set the number of ABSs to 8. The range of recharging delay is calculated based on the waiting time before being recharged, as the available stations are less than the number of waiting ABSs in the recharging state. Then, the total recharging delay curve is obtained by accumulative stacking. As seen in Figure 5.9, when the number of stations decreases, for each ABS, it is more probable to wait. As the number of stations increases from 2 to 5, the value of the mean waiting time before recharging approximately drops from 3.4 to $0.94h$. This implies that the increase on the number of stations will cause a significant decrease in the recharging delay and this mean value is improved with the proposed scheduling approach.

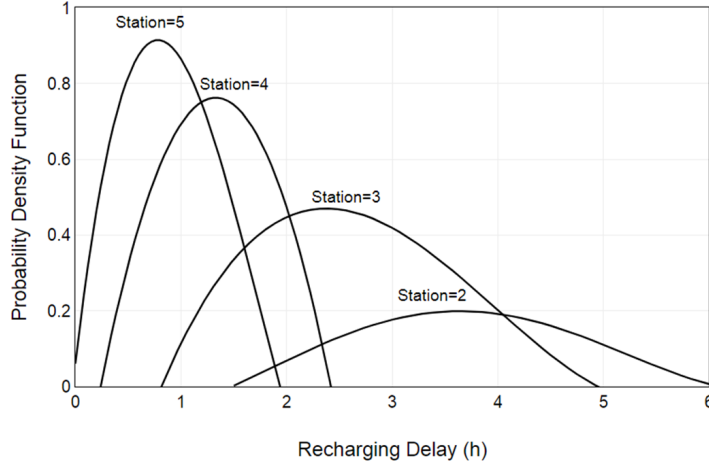


Figure 5.9 : Probability density function of recharging delay for one ABS. The number of replenishment station is equal to 5, 4, 3 and 2. The number of waiting ABSs is equal to 8.

5.5 Handover Procedure

We compare our results with the traditional handover mechanism by using the coverage model in [52]. The traditional handover mechanism focuses on the comparison of the RSRP with a constant handover threshold value. However, it is observed that users with various speeds can lead to performing some unnecessary handovers [73]. We evaluate the results in terms of handover failure ratio and handover delay where handover delay is measured as follows [49]- [74]:

$$H = (1 - \vartheta)(R_T + R_W) + \vartheta T_R \quad (5.1)$$

where ϑ is the probability of successful handover, R_T is the time to retry on the failure of a handover, R_W is the waiting time for the establishment of a handover, and T_R is the handover time. It is assumed that $R_T = 15msec$, $R_W = 20msec$ with $T_R = 30msec$. HMS is equal to $1dB$ and TTT is $40ms$.

In Figure 5.10, the handover failure ratio is shown with respect to the user density. When the user density increases in the topology, the received signal can be unstable and this causes increased handover failure. In the traditional handover mechanism, we observed that the users with various speeds cannot have the same signal quality. In addition, unnecessary handovers cause unnecessary energy consumption. With the limited battery capacity of ABSs, there is a direct impact on the flight endurance. However, handover mechanism can be intelligently managed from the perspective of

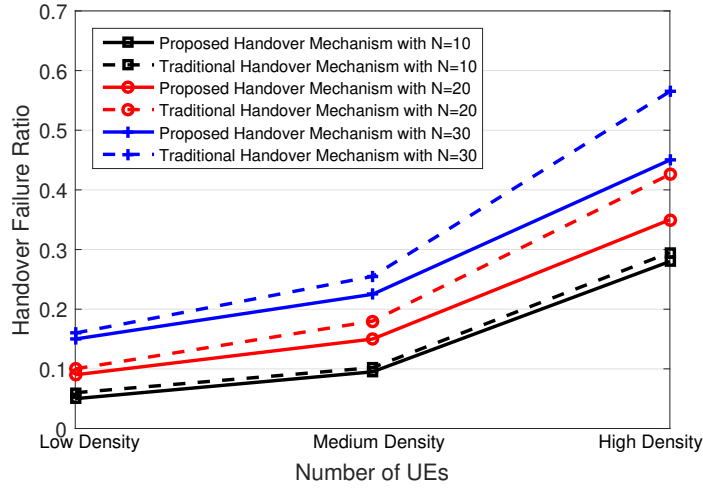


Figure 5.10 : Handover failure ratio w.r.t. user density.

a centralized control station and improved considerably by triggering the handover among ABSs. With the proposed model, we observe an average 18% decrease in handover failure ratio compared to the traditional handover mechanism.

Handover delay is shown in Figure 5.11 with 20 ABSs. As explained in Chapter 4.6.3, the number of the UEs directly affects the number of handovers that results in increasing handover delay and waiting time in the queue. However, with the proposed handover approach, we obtain almost 12% decrease in handover delay. Since the control station triggers the ABSs for handover, handover delay severely shows a degradation, in particular, there is an important decrease in high density.

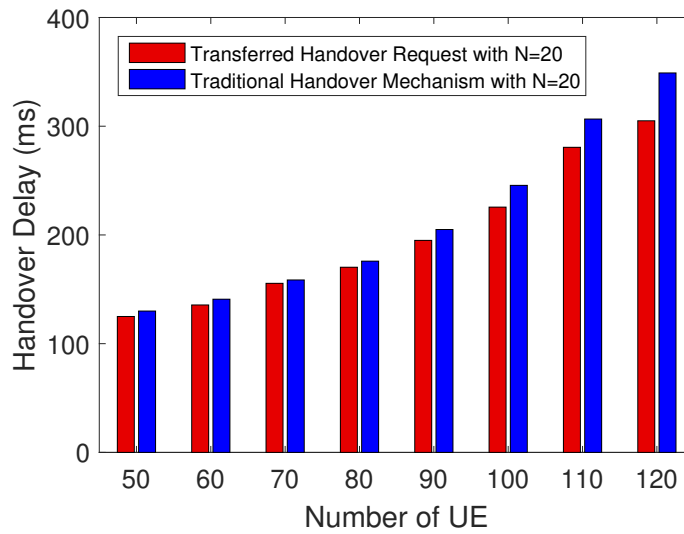


Figure 5.11 : Handover delay (ms) with 20 ABSs w.r.t. varying number of users.



6. CONCLUSION

Huge natural disasters may cause profound damage and faults in communication infrastructure. In mission critical environments, dealing with the faults and challenges is of great importance. In case of the failure of BSs, it is tremendously time-consuming to redesign the network. Reactivation of inaccessible BSs makes the topology control and connectivity a challenging task. In addition, an instant increase in traffic flows, and subsequent problems with communications caused by the huge demand of users, cannot be met by the existing infrastructure since the users may consume all of the network resources in unexpected turn of events. Therefore, existing network infrastructure needs some mechanisms to reduce possible effects after such unexpected environments.

Resilience is the ability of a system for providing an acceptable level of service to deal with faults, changes or challenges. It can be easily observed that network infrastructure will need to be modified and improved after unexpected events. Thus, communication networks should be adaptive against the changes. However, huge demand of users and the failure of the terrestrial BSs cause a degradation in resilience. To deal with the challenge, ABSs play a central role in mission critical environments due to the fast deployment, flexible reconfiguration and low cost. In this manner, through the controllable ABSs that are directed to the disaster region, users can continuously remain connected with ABSs. However, several key challenges happen with the ABS deployment to provide on-demand communication and enable "QoE-guaranteed" service to the users.

Thus, in this thesis, we first presented and evaluated *AirNet*, an energy-aware ABS deployment and scheduling mechanism accounting for replenishment stations. We addressed the problem of ABS deployment to maximize the covered UEs in an online-manner. In particular, *AirNet*'s operation is demand-aware and accounts for time-varying user requests. We also demonstrated, using an energy model, how an efficient algorithm can increase the flight endurance. Furthermore, we presented a

scheduling algorithm for battery recharging under the constraint of a limited number of replenishment stations. Our simulations also confirm the effectiveness of the proposed algorithms in terms of user coverage and flight endurance. In particular, our results indicate that *AirNet* can achieve a 24% improvement in user coverage and an 8% extension in flight endurance.

Then, this thesis addressed the problem of continuous movement control of ABSs for providing communication coverage and handover management. We investigated the existing handover solutions that are not optimized for supporting aerial networks and thus are facing new challenges. Therefore, we analyzed the handover delay and handover failure ratio proposing a solution. Simulation results show that the proposed energy-aware approach can achieve at least 12% and 18% improvements concerning handover delay and handover failure ratio compared to a traditional approach.

We see our work as a first step and believe that it opens several interesting avenues for future research. In particular, we so far assumed a relatively simple model for the to-be-covered area, and it would be interesting to investigate more complex scenarios, e.g., due to mountains or other obstructions. It would also be interesting to consider the use of randomized algorithms.

REFERENCES

- [1] http://www.soumu.go.jp/main_sosiki/joho_tsusin/eng/pdf/110729_1.pdf.
- [2] **Holling, C.** (1973). Resilience and stability of ecological systems, *Annual Review of Ecology and Systematics*, 4(1), 1–23.
- [3] **Godschalk, D.** (2003). Urban hazard mitigation: Creating resilient cities, *Natural Hazards Review*, 4(1), 136–143.
- [4] **J. P. G. Sterbenz, D. Hutchison, E.K.C.A.J.J.P.R.M.S. and Smith, P.** (2010). Resilience and survivability in communication networks: Strategies, principles, and survey of disciplines, *Computer Networks: Special Issue on Resilient and Survivable Networks*, 54(8), 1245–1265.
- [5] **Kazama, M. and Noda, T.** (2012). Damage statistics (Summary of the 2011 off the Pacific Coast of Tohoku Earthquake damage), *The Japanese Geotechnical Society, Soils and Foundations*, 52(5), 780–792.
- [6] **Iqbal, H., Ma, J., Stranc, K., Palmer, K. and Benbenek, P.** (2016). A software-defined networking architecture for aerial network optimization, *2016 IEEE NetSoft Conference and Workshops (NetSoft)*, pp.151–155.
- [7] 3GPP, Technical Specification Group Radio Access Network, Study on Enhanced LTE Support for Aerial Vehicles (Release 15), TR 36.777 V15.0.0, *John Wiley & Sons Ltd*.
- [8] **Bai, J., Yeh, S., Xue, F. and Talwar, S.** (2019). Route-Aware Handover Enhancement for Drones in Cellular Networks, *2019 IEEE Global Communications Conference (GLOBECOM)*, pp.1–6.
- [9] Companion Volume to Weather, Climate & Catastrophe Insight, Additional Data to Accompany the 2017 Annual Report, <http://thoughtleadership.aonbenfield.com/Documents/20180124-ab-if-annual-companion-volume.pdf>.
- [10] Cisco Visual Networking Index: Forecast and Trends, 2017–2022, <https://cyrekdigital.com/pl/blog/content-marketing-trendy-na-rok-2019/white-paper-cll-741490.pdf>.
- [11] **P. H. Longstaff, S.Y.** (2008). Communication Management and Trust: Their Role in Building Resilience to “Surprises” Such as Natural Disasters, Pandemic Flu, and Terrorism, *Ecology and Society*, 13(1).

- [12] **P. Smith, D. Hutchison, J.P.G.S.M.S.A.F.M.K.B.P.** (2011). Network Resilience: A Systematic Approach, *IEEE Communications Magazine*, 49(7), 88–97.
- [13] **Izaddoost, A. and Heydari, S.** (2014). Proactive Risk Mitigation for Communication Network Resilience in Disaster Scenarios, *IEEE 15th International Symposium on World of Wireless, Mobile and Multimedia Networks (WoWMoM)*.
- [14] **P. Cholda, A. Mykkeltveit, B.E.H.O.J.W.A.J.** (2007). A Survey of Resilience Differentiation Frameworks in Communication Networks, *IEEE Communications Surveys and Tutorials*, 9(4), 32–55.
- [15] **N.H.Motlagh, T.Taleb, O.** (2016). Low-Altitude Unmanned Aerial Vehicles-based Internet of Things Services: Comprehensive Survey and Future Perspectives, *IEEE Internet of Things Journal*, 3(6), 899–919.
- [16] http://cordis.europa.eu/project/rcn/206640_en.html.
- [17] <http://www.rescuecell.eu/>.
- [18] <http://www.sherpa-project.eu/sherpa/>.
- [19] https://wiki.ittc.ku.edu/resilinet/Main_Page.
- [20] <http://www.resist-catreneproject.eu/home/>.
- [21] **S. Waharte, N.T. and Julier, S.** (2009). Coordinated search with a swarm of UAVs, *IEEE Sensor Mesh Ad Hoc Communication Networks Workshops*.
- [22] **Ruan, L., Wang, J., Chen, J., Xu, Y., Yang, Y., Jiang, H., Zhang, Y. and Xu, Y.** (2018). Energy-efficient multi-UAV coverage deployment in UAV networks: A game-theoretic framework, *China Communications*, 15, 194–209.
- [23] **Li, B., Chen, C., Zhang, R., Jiang, H. and Guo, X.** (2018). The Energy-Efficient UAV-Based BS Coverage in Air-to-Ground Communications, *2018 IEEE 10th Sensor Array and Multichannel Signal Processing Workshop (SAM)*, pp.578–581.
- [24] **Alzenad, M., El-Keyi, A., Lagum, F. and Yanikomeroglu, H.** (2017). 3-D Placement of an Unmanned Aerial Vehicle Base Station (UAV-BS) for Energy-Efficient Maximal Coverage, *IEEE Wireless Communications Letters*, 6(4), 434–437.
- [25] **Azari, M.M., Rosas, F., Chen, K. and Pollin, S.** (2018). Ultra Reliable UAV Communication Using Altitude and Cooperation Diversity, *IEEE Transactions on Communications*, 66(1), 330–344.
- [26] **Lee, H.S., Yoo, H.W. and Lee, B.H.** (2015). Deployment method of UAVs with energy constraint for multiple tasks, *Electronics Letters*, 51(21), 1650–1652.

- [27] **Kandeepan, S., Gomez, K., Reynaud, L. and Rasheed, T.** (2014). Aerial-terrestrial communications: terrestrial cooperation and energy-efficient transmissions to aerial base stations, *IEEE Transactions on Aerospace and Electronic Systems*, 50(4), 2715–2735.
- [28] **Merwaday, A., Tuncer, A., Kumbhar, A. and Guvenc, I.** (2016). Improved Throughput Coverage in Natural Disasters: Unmanned Aerial Base Stations for Public-Safety Communications, *IEEE Vehicular Technology Magazine*, 11(4), 53–60.
- [29] **Mozaffari, M., Saad, W., Bennis, M. and Debbah, M.** (2017). Wireless Communication Using Unmanned Aerial Vehicles (UAVs): Optimal Transport Theory for Hover Time Optimization, *IEEE Transactions on Wireless Communications*, 16(12), 8052–8066.
- [30] **Monwar, M., Semiari, O. and Saad, W.** (2018). Optimized Path Planning for Inspection by Unmanned Aerial Vehicles Swarm with Energy Constraints, *CoRR*, abs/1808.06018, <http://arxiv.org/abs/1808.06018>, 1808.06018.
- [31] **Mardani, A., Chiaberge, M. and Giaccone, P.** (2019). Communication-Aware UAV Path Planning, *IEEE Access*, 7, 52609–52621.
- [32] **Wu, J., Yu, P., Feng, L., Zhou, F., Li, W. and Qiu, X.** (2019). 3D Aerial Base Station Position Planning based on Deep Q-Network for Capacity Enhancement, *2019 IFIP/IEEE Symposium on Integrated Network and Service Management (IM)*, pp.482–487.
- [33] **Xiao, Z., Zhu, B., Wang, Y. and Miao, P.** (2018). Low-Complexity Path Planning Algorithm for Unmanned Aerial Vehicles in Complicated Scenarios, *IEEE Access*, 6, 57049–57055.
- [34] **Tao, J., Zhong, C., Gao, L. and Deng, H.** (2016). A Study on Path Planning of Unmanned Aerial Vehicle Based on Improved Genetic Algorithm, *2016 8th International Conference on Intelligent Human-Machine Systems and Cybernetics (IHMSC)*, volume 02, pp.392–395.
- [35] **Foo, J., Knutzon, J., Kalivarapu, V., Oliver, J. and Winer, E.** (2009). Path Planning of Unmanned Aerial Vehicles Using B-Splines and Particle Swarm Optimization, *Journal of Aerospace Computing Information and Communication*, 6, 271–290.
- [36] **Bekhti, M., Abdennebi, M., Achir, N. and Boussetta, K.** (2016). Path planning of unmanned aerial vehicles with terrestrial wireless network tracking, *2016 Wireless Days (WD)*, pp.1–6.
- [37] **Vazirani, V.V.** (2003). Approximation Algorithms, *Springer*, pp.1–389.
- [38] **Biniiaz, A., Liu, P., Maheshwari, A. and Smid, M.** (2016). Approximation algorithms for the unit disk cover problem in 2D and 3D, *Computational Geometry*, 60.

- [39] **Gao, X., Fan, J., Wu, F. and Chen, G.** (2018). Approximation Algorithms for Sweep Coverage Problem With Multiple Mobile Sensors, *IEEE/ACM Transactions on Networking*, 26(2), 990–1003.
- [40] **Ren, Y., Li, Y. and Qi, C.** (2017). Handover Rate Analysis for K-Tier Heterogeneous Cellular Networks With General Path-Loss Exponents, *IEEE Communications Letters*, 21(8), 1863–1866.
- [41] **Yusof, A.L., Ali, M.S.N. and Ya’acob, N.** (2019). Handover Implementation for Femtocell Deployment in LTE Heterogeneous Networks, *2019 International Symposium on Networks, Computers and Communications (ISNCC)*, pp.1–5.
- [42] **Alotaibi, N.M. and Alwakeel, S.S.** (2015). A Neural Network Based Handover Management Strategy for Heterogeneous Networks, *2015 IEEE 14th International Conference on Machine Learning and Applications (ICMLA)*, pp.1210–1214.
- [43] **Vasudeva, K., Simsek, M., López-Pérez, D. and Güvenç, (2017).** Analysis of Handover Failures in Heterogeneous Networks With Fading, *IEEE Transactions on Vehicular Technology*, 66(7), 6060–6074.
- [44] **Park, K., Cho, B., Park, K. and Kim, H.** (2015). Optimal coverage control for net-drone handover, *2015 Seventh International Conference on Ubiquitous and Future Networks*, pp.97–99.
- [45] **Huang, W., Zhang, H. and Zhou, M.** (2019). Analysis of Handover Probability Based on Equivalent Model for 3D UAV Networks, *2019 IEEE 30th Annual International Symposium on Personal, Indoor and Mobile Radio Communications (PIMRC)*, pp.1–6.
- [46] **Hu, B., Yang, H., Wang, L. and Chen, S.** (2019). A trajectory prediction based intelligent handover control method in UAV cellular networks, *China Communications*, 16(1), 1–14.
- [47] **Hong, T.C., Kang, K., Lim, K., Lee, B. and Ahn, J.Y.** (2017). Signal transmission method for measurement used in handover of control and non-payload communication of unmanned aerial vehicle, *2017 International Conference on Information and Communication Technology Convergence (ICTC)*, pp.5–7.
- [48] **Arshad, R., Elsayy, H., Lampe, L. and Hossain, M.J.** (2019). Handover Rate Characterization in 3D Ultra-Dense Heterogeneous Networks, *IEEE Transactions on Vehicular Technology*, 68(10), 10340–10345.
- [49] **Sharma, V., Song, F., You, I. and Chao, H.** (2017). Efficient Management and Fast Handovers in Software Defined Wireless Networks Using UAVs, *IEEE Network*, 31(6), 78–85.
- [50] **Banagar, M., Chetlur, V.V. and Dhillon, H.S.** (2020). Handover Probability in Drone Cellular Networks, *IEEE Wireless Communications Letters (Early Access)*.

- [51] **Moradi, M., Sundaresan, K., Chai, E., Rangarajan, S. and Mao, Z.M.** (2018). SkyCore: Moving Core to the Edge for Untethered and Reliable UAV-Based LTE Networks, *Proceedings of the 24th Annual International Conference on Mobile Computing and Networking, MobiCom '18*, Association for Computing Machinery, New York, NY, USA, p.35–49, <https://doi.org/10.1145/3241539.3241549>.
- [52] **Mozaffari, M., Saad, W., Bennis, M. and Debbah, M.** (2016). Efficient Deployment of Multiple Unmanned Aerial Vehicles for Optimal Wireless Coverage, *IEEE Communications Letters*, 20(8), 1647–1650.
- [53] **Al-Hourani, A., Kandeepan, S. and Lardner, S.** (2014). Optimal LAP Altitude for Maximum Coverage, *IEEE Wireless Communications Letters*, 3(6), 569–572.
- [54] **Bor-Yaliniz, I. and El-Keyi, A.** (2016). Efficient 3-D Placement of an Aerial Base Station in Next Generation Cellular Networks, *IEEE International Conference on Communications (ICC)*.
- [55] **Al-Hourani, A., Kandeepan, S. and Jamalipour, A.** (2014). Modeling air-to-ground path loss for low altitude platforms in urban environments, *2014 IEEE Global Communications Conference*, pp.2898–2904.
- [56] (2018). Small Unmanned Aircraft Regulations (Part 107), *Code of Federal Regulations, Title 14 Aeronautics and Space, Parts 60 to 109*.
- [57] **Ghazzai, H., Ben Ghorbel, M., Kadri, A., Hossain, M.J. and Menouar, H.** (2017). Energy-Efficient Management of Unmanned Aerial Vehicles for Underlay Cognitive Radio Systems, *IEEE Transactions on Green Communications and Networking*, 1(4), 434–443.
- [58] **Hulens, D., Verbeke, J. and Goedemé, T.** (2015). How to Choose the Best Embedded Processing Platform for on-Board UAV Image Processing, *International Joint Conference Computer Vision, Imaging and Computer Graphics Theory and Applications (VISIGRAPP)*.
- [59] <http://thoughtleadership.aonbenfield.com/Documents/20180124-ab-if-annual-companion-volume.pdf>.
- [60] <http://ardupilot.org/dev/docs/sitl-native-on-windows.html>.
- [61] **D'Hondt, V.** (1878). La representation proportionnelle des parties.
- [62] **D'Hondt, V.** (1882). Systeme pratique et raisonne de representation proportionnelle.
- [63] **Gross, D., Shortle, J.F., Thompson, J.M. and Harris, C.M.** (2008). Fundamentals of Queueing Theory, *Fourth Edition, A John wiley & Sons, Inc., Publication*.
- [64] **Gupta, L., Jain, R. and Vaszkun, G.** (2016). Survey of Important Issues in UAV Communication Networks, *IEEE Communications Surveys Tutorials*, 18(2), 1123–1152.

- [65] **Sutton, R.S. and Bartoc, A.G.** (2017). Reinforcement Learning: An Introduction, *The MIT Press Cambridge, Massachusetts, London, England*.
- [66] **Watkins, C.J.C.H.** (1989). Learning from Delayed Rewards, *Ph.D. thesis, Cambridge University*.
- [67] **Hu, R.Q. and Qian, Y.** (2013). Heterogeneous Cellular Networks, *John Wiley & Sons Ltd*.
- [68] **Bilen, T., Canberk, B. and Chowdhury, K.R.** (2017). Handover Management in Software-Defined Ultra-Dense 5G Networks, *IEEE Network*, 31(4), 49–55.
- [69] **Kleinrock, L.** (1975). Queueing Systems, Vol.1: Theory, A *Wiley-Interscience Publication, John Wiley & Sons*.
- [70] **Aydin, O., Malanchini, I. and Gebert, J.** (2016). Seamless replacement of a first drone base station with a second drone base station.
- [71] 3GPP TS 36.423: LTE, Evolved Universal Terrestrial Radio Access Network (E-UTRAN), X2 Application Protocol (X2AP).
- [72] **Nurmela, K.J. and Ostergar, P.R.J.** (2000). Covering Square with up to 30 Equal Circles, *Helsinki University of Technology, Laboratory for Theoretical Computer Science*.
- [73] **Zhang, H., Wen, X., Wang, B., Zheng, W. and Sun, Y.** (2010). A Novel Handover Mechanism Between Femtocell and Macrocell for LTE Based Networks, *2010 Second International Conference on Communication Software and Networks*, pp.228–231.
- [74] **Yang, B., Wu, Y., Chu, X. and Song, G.** (2016). Seamless Handover in Software-Defined Satellite Networking, *IEEE Communications Letters*, 20(9), 1768–1771.

APPENDICES

APPENDIX A: Proof of Approximations





APPENDIX A: Proof of Approximations

In Algorithm 2, we initially select M-sets that maximize the number of covered UEs. Here, OPT shows the optimal solution to maximize the covered UEs. Let us denote a_i as the number of newly covered UEs, b_i as the total number of UEs and c_i as the number of uncovered UEs at the i_{th} iteration so that $b_i = \sum_{j=1}^i a_j$ and $c_i = OPT - b_i$ [59].

The number of newly covered UEs at the $(i+1)_{th}$ iteration is equal to or greater than $1/M$ of the number of uncovered UEs after i_{th} iteration such that $a_{i+1} \geq \frac{c_i}{M}$.

Lemma: $c_{i+1} \leq (1 - \frac{1}{M})^{i+1} \cdot OPT$

Proof: By induction, we give the steps for $i = 0$ [59].

$$\begin{aligned}
 c_1 &\leq \left(1 - \frac{1}{M}\right) OPT \\
 OPT - b_1 &\leq OPT - OPT \frac{1}{M} \\
 b_1 &\geq OPT \frac{1}{M} \\
 a_1 &\geq OPT \frac{1}{M} \\
 a_1 &\geq c_0 \frac{1}{M}
 \end{aligned} \tag{A.1}$$

Then, we know $a_1 \geq c_0 \frac{1}{M}$ for $i = 0$. Assume $c_i \leq (1 - \frac{1}{M})^i OPT$ is true, we show that $c_{i+1} \leq (1 - \frac{1}{M})^{i+1} OPT$ is true [59].

$$\begin{aligned}
 c_{i+1} &= c_i - a_{i+1} \\
 c_{i+1} &\leq c_i - \frac{c_i}{M} \\
 c_{i+1} &\leq c_i \left(\frac{1}{M}\right) \\
 c_{i+1} &\leq \left(\frac{1}{M}\right)^i OPT \left(1 - \frac{1}{M}\right) \\
 c_{i+1} &\leq \left(\frac{1}{M}\right)^{i+1} OPT
 \end{aligned} \tag{A.2}$$

Theorem: A greedy algorithm achieves a $(1 - \frac{1}{e})$ approximation factor [59].

Proof: By Lemma 1, we know that $c_M \leq (1 - \frac{1}{M})^M OPT$. Then, $(1 - \frac{1}{M})^M \approx \frac{1}{e}$ so that $c_M \leq \frac{OPT}{e}$ [59].

$$\begin{aligned}
 b_M &= OPT - c_M \\
 b_M &= OPT - \frac{OPT}{e} \\
 b_M &= OPT \left(1 - \frac{1}{e}\right)
 \end{aligned} \tag{A.3}$$



CURRICULUM VITAE

Name Surname: Elif BOZKAYA

Place and Date of Birth: İzmit, Turkey, 01 January 1988

E-Mail: bozkayae@itu.edu.tr

EDUCATION:

- **M.Sc.:** 2015, Istanbul Technical University, Faculty of Computer and Informatics, Department of Computer Engineering, Computer Engineering Programme
- **B.Sc.:** 2009, National Defense University Naval Academy, Department of Computer Engineering, Computer Engineering Programme

PROFESSIONAL EXPERIENCE:

- 2016-present, Lecturer at National Defense University Naval Academy, Department of Computer Engineering.
- 2019, Visiting Researcher at University of Vienna, Austria
- 2019-present, Reviewer for journal: IEEE Transactions on Vehicular Technology.
- 2019-present, Reviewer for journal: IEEE Communications Letters
- 2017-present, Reviewer for journal: Elsevier Computer Communications.
- 2017-present, Reviewer for journal: IEEE Transactions on Wireless Communications
- 2016-present, Reviewer for journal: Elsevier Ad Hoc Networks.
- 2014-present, Reviewer for journal: The International Journal of Communication Systems (IJCS).
- 2014-present, Reviewer for journal: Elsevier Computer Networks.
- 2015-present, Reviewer for several international/national conferences: 2020 IEEE International Conference on Computer Communications (INFOCOM) Workshop on WiSARN: International Workshop on Wireless Sensor, Robot and UAV Networks, 16th Annual IEEE International Conference on Sensing, Communication, and Networking (SECON 2019), Second International Balkan Conference on Communications and Networking 2018 (BalkanCom'18), 2018 International Conference on Computing, Networking and Communications (ICNC): Internet Services and Applications, 2017 IEEE International Conference

on Communications (ICC), 2017 IEEE Wireless Communications and Networking Conference (WCNC), 41st Annual IEEE Conference on Local Computer Networks, 2016, IEEE 82nd Vehicular Technology Conference (VTC2015-Fall).

PUBLICATIONS ON THE THESIS:

- **E. Bozkaya**, B. Canberk, "SDN-enabled Deployment and Path Planning of Aerial Base Stations", *Computer Networks (Elsevier)*, vol. 171, April 2020.
- **E. Bozkaya**, K. T. Foerster, S. Schmid, B. Canberk, "*AirNet: Energy-Aware Deployment and Scheduling of Aerial Networks*", *submitted for journal publication*.
- **E. Bozkaya**, Y. Ozcevik, B. Canberk, "Energy-Aware Handover Management for Aerial Networks: A Reinforcement Learning Approach", *submitted for journal publication*.
- **E. Bozkaya**, B. Canberk, "BS-on-Air: Optimum UAV Localization for Resilient Ultra Dense Networks", in *IEEE International Workshop on Wireless Sensor, Robot and UAV Networks, IEEE International Conference on Computer Communications Communications (IEEE INFOCOM)*, Hawaii-USA, April 2018.

OTHER PUBLICATIONS:

- S. Mohanti, **E. Bozkaya**, M. Y. Naderi, B. Canberk and K. R. Chowdhury, "WiFED: WiFi Friendly Energy Delivery with Distributed Beamforming", in *IEEE Conference on Computer Communications (IEEE INFOCOM)*, Hawaii-USA, April 2018, (Best Paper Award).
- **E. Bozkaya**, B. Canberk, "Software-Defined Management Model for Energy-Aware Vehicular Networks", *EAI Endorsed Transactions on Wireless Spectrum*, vol. 3, pp.11-17, January 2017.
- **E. Bozkaya**, B. Canberk, "Robust and Continuous Connectivity Maintenance for Vehicular Dynamic Spectrum Access Networks", *Ad Hoc Networks Journal (Elsevier)*, vol. 5, part A, pp. 72-83, February 2015.
- **E. Bozkaya**, M. Erel, B. Canberk, "Connectivity Provisioning Using Cognitive Channel Selection in Vehicular Networks", *Lecture Notes of the Institute of Computer Sciences, Social Informatics and Telecommunications Engineering, Ad Hoc Networks (Springer)*, vol. 140, pp. 169-179, November 2014.
- **E. Bozkaya**, B. Canberk, "Crowdsourcing Applications for Vehicular Social Networks", *Vehicular Social Networks, Edited by A. M. Vegni, V. Loscri and A.V. Vasilakos*, CRC Press, 2017.
- **E. Bozkaya**, B. Canberk, "Connectivity Analysis and Modelling in Cognitive Vehicular Networks", *Cognitive Vehicular Networks*, Edited by A. M. Vegni and D. P. Agrawal, CRC Press, 2015.
- **E. Bozkaya**, K. R. Chowdhury, B. Canberk, "SINR and Reliability based Hidden Terminal Estimation for Next Generation Vehicular Networks", in *12th ACM International Symposium on QoS and Security for Wireless and Mobile Networks (ACM Q2SWiNET)*, Valletta-MALTA, November 2016.

- **E. Bozkaya**, B.Canberk, "QoE-based Flow Management in Software Defined Vehicular Networks", in *IEEE International Workshop on Advances in Software Defined Radio Access Networks and Context-Aware Cognitive Network, IEEE Global Communications Conference (IEEE GLOBECOM)*, San Diego-USA, December 2015.



